RICE UNIVERSITY

Engineering the Production of Itaconic Acid in *Escherichia coli*

by

Tao Lin

A THESIS SUBMITTED IN PARTIAL FULFILLMENT OF THE REQUIREMENTS FOR THE DEGREE

Master of Science

APPROVED, THESIS COMMITTEE

George Bennett, Thesis Director
E. D. Butcher Professor, Biochemistry and Cell Biology

Kathleen M. Beckingham, Committee Chair
Professor, Biochemistry and Cell Biology

Ka-Yiu San, E. D. Butcher Professor in Bioengineering and Professor of Chemical Engineering

Michael C. Gustin, Professor, Biochemistry and Cell Biology

Ronald Parry, Professor of Chemistry and Professor of Biochemistry and Cell Biology

HOUSTON, TEXAS
Jan 2011

Abstract

Engineering the Production of Itaconic Acid in *Escherichia coli*

by

Tao Lin

Itaconic acid (IA) has many versatile applications in science and medicine. Engineering *Escherichia coli* can provide a reliable route for IA production, where *cis*-aconitate decarboxylase (CAD) is one essential enzyme in the process. The synthetic *cad* gene has been cloned into various vectors to improve the expression rate and folding activities. The strain bearing plasmid pTrc99a-*cad* displays a significant amount of IA production, while the CAD protein expressed from the same plasmid displays the highest enzymatic activity in vitro. To improve the reliability of forming the *cis*-aconitate intermediate, the aconitase genes from *Aspergillus terreus* have been cloned into the pTrc99a vector. The expression of aconitate hydratase leads to a peak at 10.3 min in the HPLC spectra after 4 hours incubation. The peak will be analyzed to determine whether it is *cis*-aconitate. The obtained data will provide data on possible metabolic pathways of IA production in *Aspergillus terreus.*

Acknowledgments

First of all, I would like to sincerely thank my advisor, Dr. George Bennett, for his steady support, guidance, and advice all the time. His wisdom and encouragement kept motivating me through the good and tough times during the research.

Secondly, I would like to thank my committee members, Dr. Kathleen Beckingham, Dr. Michael Gustin, and Dr. Ka-Yiu San for their advice and suggestions during the research progress. Their brilliant suggestions ease the difficulties of the research and contributed significantly to my research. Additionally, I need to thank Dr. Ronald Parry to serve in my thesis committee.

Thirdly, I have to thank my colleagues in Drs. Bennett and San labs for their help and advice: Xianpeng, Chandresh, Yipeng, Huasong, Mary, Jiangfeng, Mai, Xiuzhun, and Haijun, Apita, and Grant. Xianpeng helped me initiate my project. The rest of my colleagues taught me many useful molecular biology techniques and guide me through many obstacles during the research. Additionally, I need to thank specially to Mary Harrison and Dr. Zhang. Mary is always ready to help me and comfort me during the research. Dr. Zhang helped me a lot in cloning the genes from *Aspergillus terreus.*

Fourthly, I would like to present my gratitude to Dr. Greg May and his lab members in M.D. Anderson Cancer Center. Their expertise in *Aspergillus* fungi has made great contribution to my research. I really appreciate their help.

Finally, I need to thank my parents and my brother for their full support during the research. Their encouragement motivated me during my research.

The project is supported by Shell Sustainability Grant.

Table of Contents

List of Figures

List of Tables

List of Abbreviation

µg	microgram
A. niger	*Aspergillus niger*
A. terreus	*Aspergillus terreus*
Acn	aconitase
acnA	aconitase A
acnB	aconitase B
AcnD	Aconitase D
Ap	ampicillin
BLAST	Basic Local Alignment Search Tool
CAD	*cis*-aconitate decarboxylase
cad	*cis*-aconitate decarboxylase gene
cDNA	complementary DNA
CM	complete medium
Cm	chloramphenicol
DNA	deoxyribonucleic acid
DTT	dithiothreitol

E. coli	*Escherichia coli*
EDTA	ethylene diamine-tetraacetic acid
EMP	Embden-Meyerhof-Parnas
HEAT	Hungtingtin-Elongation-A subunit-TOR
HPLC	high pressure liquid chromatography
IA	itaconic acid
IPMI	isopropylmalate isomerases
IPTG	isopropyl-β-D-thiogalactoside
IRP	iron regulatory protein
kDa	kilodalton
LB	Luria broth
mAcn	mitochondrial aconitase
mAcn-ita	mitochondrial aconitase expressed in the phase of itaconic acid production
mAcn-non	mitochondrial aconitase expressed in the growth phase
Min	minutes
PCR	polymerase chain reaction
PMSF	phenylmethanesulfonylfluoride

TAE	Tris-acetate
TCA	tricarboxylic acid
X-gal	5-bromo-4-chloro-3-indolyl-β-galactoside

CHAPTER 1 Introduction

1.1 Overview

The main purpose of my study is to utilize various techniques in molecular biology, such as cloning, enzymatic assays, and shake flash fermentation, to analyze and enhance the production of useful biomolecular compounds. In particular, my study concentrates on engineering *Escherichia coli (E. coli)* to generate itaconic acid (IA) by introducing the exotic genes from *Aspergillus terreus (A. terreus)*. Previous research has shown that *cis*-aconitate decarboxylase (CAD) from *A. terreus* is one key enzyme to catalyze the conversion of *cis*-aconitate to IA; hereby, my goal is to over-express synthetic *cad* gene in *E. coli* strains. To bolster the availability of *cis*-aconitate, the aconitase (*acn)* genes from *A. terreus* are introduced and analyzed in *E. coli* strains. Various vectors would be employed to examine expression of these genes. By analyzing the metabolites produced, as well as enzymatic activities of genes in these vectors, I could investigate production of IA in *E. coli.*

1.2 Project Objectives

The primary objective of this study was the application of strategic pathway design to improve the production of itaconic acid in *E. coli.* As shown in Figure 1.1, the initial approach was to over-express the *cad* gene by cloning this gene in various vectors and analyzing the enzymatic activities both in vivo and in vitro. High activity and quantity of CAD protein would enhance the conversion of *cis*-aconitate into itaconate. This expectation would require sufficient amount of *cis*-aconitate to be accumulated inside the cytoplasm. But the aconitases in *E. coli* usually bind *cis*-aconitate inside their active sites without releasing this intermediate in the TCA cycle. Therefore, the introduction of an exotic aconitase from *A. terreus* was necessary to boost

the supply of *cis*-aconitate. Four potential aconitase genes from *A. terreus* were identified through BLASTing *Aspergillus niger* 318.55 aconitase genes with the entire genomic DNA of *A. terreus NIH2426.* Testing these potential aconitase genes might allow us to identify a unique aconitase that specifically converts citrate into *cis*-aconitate, increasing the supply of the intermediate. Beyond cloning these genes, I also planned to delete the branch pathways of pyruvate and acetyl-CoA to increase the flux of oxaloacetate. As a result, these actions would be expected to improve the production of IA.

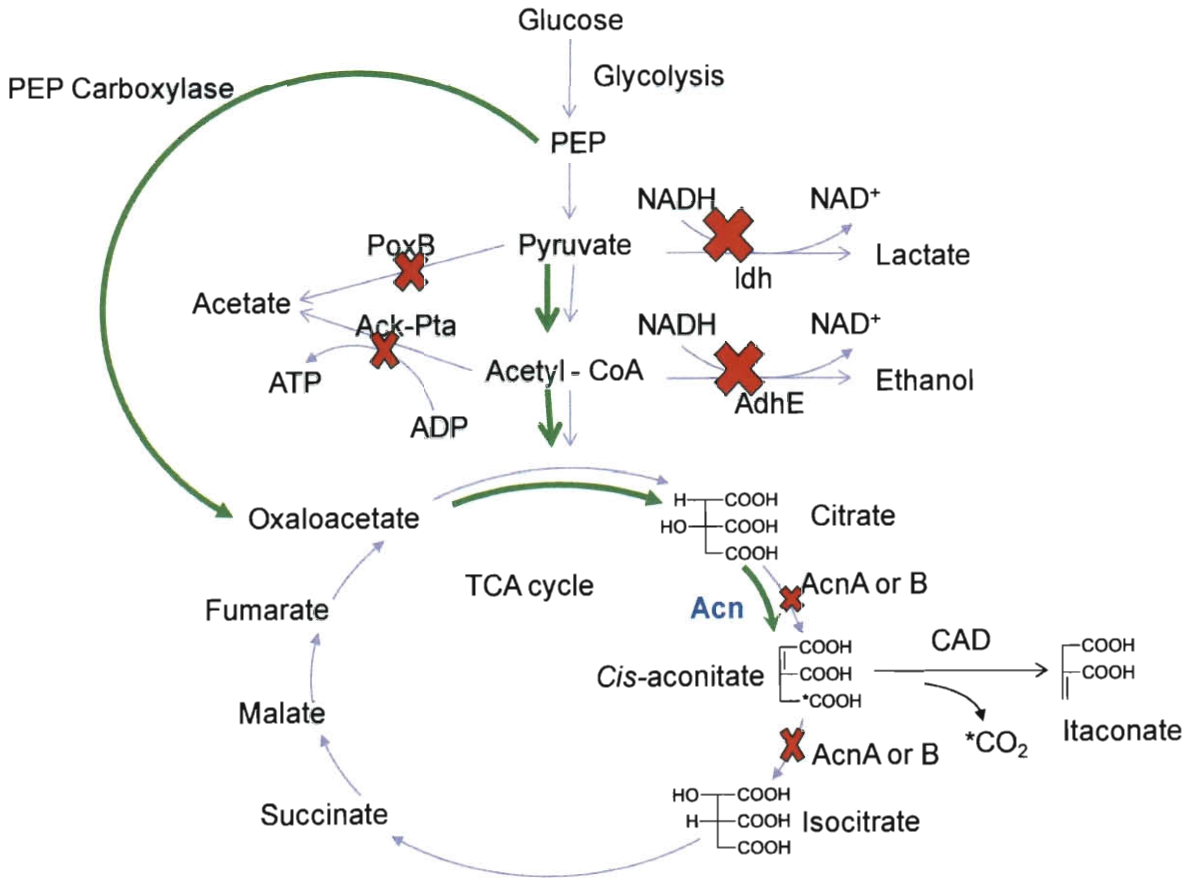

Figure 1.1 – Proposed strategy to increase the main flux of glycolysis and the TCA cycle in *E. coli.*

✖ --Gene knockout; ⟶ -- the increased flux of pathway; **Acn** – aconitase from other species.

1.3 Background

1.3.1 Characteristics and applications of IA

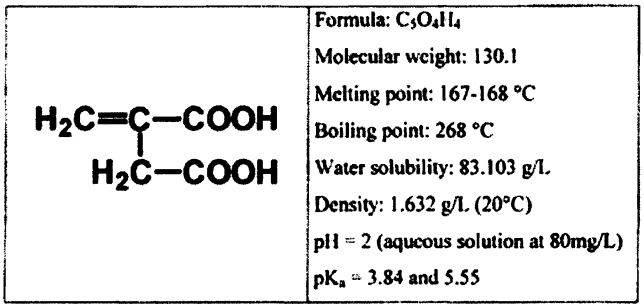

Figure 1.2 – The structure and properties of itaconic acid (Willke and Vorlop, 2001)

Itaconic acid (IA) is a white crystalline dicarboxylic acid with the double bond that is conjugated to one carboxyl group (See Figure 1.2) (Willke and Vorlop, 2001). Its characteristics and potential reactions have been well reviewed by Tate (Tate, 1970). The double bond structure enables IA to be easily polymerized to form sophisticated complexes, while the two carboxyl groups contribute to effective acidic functionality. These characteristics allow IA to serve in many versatile applications in industry, agriculture, pharmacy, and medicine (Okabe et al., 2009). For instance, the polymerized methyl, ethyl, or vinyl forms of itaconate have been widely used in oral drug-delivery (Betancourt et al.; Teijon et al., 2009), dental glass-ionomer cements (Coutinho et al., 2009; Moshaverinia et al., 2009), water resistant resins (Zhao et al., 2004), and so on. The common detergents, cleaners, and other related products also utilize IA in their ingredients (Lancashire, 1969). Furthermore, with the depletion of petroleum resources, IA can substitute for petroleum derived products, such as acrylic or methylacrylic acid (Willke and Vorlop, 2001), and also serve as a precursor for many useful chemicals (Ltd, 2008). Thus, the investigations into new properties of IA have provided more possibilities for novel applications

in various fields. IA has been categorized as one of the twelve most important renewable chemicals by the United States Department of Energy (Ltd, 2008). Each year, more than eighty thousand tons of IA are produced in the world (Okabe et al., 2009). Although the price of IA has dropped from $4.3 US dollars (Willke and Vorlop, 2001) to $2 US dollars per kilogram (Okabe et al., 2009) in ten years, the continuously growing market demands the production of IA with higher efficiency and lower production costs.

1.3.2 Industrial production of IA and IA producing strains

Chemical synthesis methods for IA have been developed since 1943 (Blatt, 1943), but none of these processes has been practiced commercially due to expensive production costs. Instead, the main route for production of IA is via fermentation of *A. terreus*. Since the first plant was established by Pfizer Co. Inc. (Pfeifer et al., 1952), many efforts have been made to optimize the production of IA on a large scale, including strain selections, fermentation process manipulations, various substrate utilizations, and so on (Okabe et al., 2009). For instance, Yahiro et al. treated the parent strain, *A. terreus* IFO-6365, with N-Methyl-*N'*-nitro-*N*-nitrosoguanidine (NTG) and selected the high-producing strain, A. *terreus* TN-484-M1. The selected stain can produce 82 g/l of IA from 160 g/l of glucose in a shaking flask in 6 days (Yahiro et al., 1995). To improve the economics of fermentation processes, various kinds of bioreactors have been tested to compete for the higher efficiency of IA production, including bubble column, packed bubble column, tubular reactor, and air-lift reactor (Okabe et al., 2009). Moreover, other inexpensive alternative feedstocks, such as corn steep liquor and glycerol (Jarry and Seraudie, 1995), have been reported in industrial fermentations to further reduce costs. Although *A. terreus* has been commonly used in commerce, many other organisms have been explored for the production of IA. For instance, *Aspergillus itaconicus* was first isolated to produce IA for industrial uses

(Kinoshita, 1932). *Ustilago* and *Candida* species also produce IA from glucose (Panakova, 2009; Tabuchi, 1991, 1980; Tabuchi et al., 1981). In this project, we are interested in exploring the possibilities of *E. coli* for IA production.

1.3.3 Metabolic pathway of IA production in *A. terreus*

To engineer *E. coli* to produce IA, it is essential to understand the biosynthesis of IA in fungi. For decades, scientists proposed various theories of IA production in fungal cells (Bentley and Thiessen, 1957a; Eimhjellen and Larsen, 1955; Kinoshita, 1932; Shimi and Nour El Dein, 1962). Most accumulated evidence supports that the production of IA is mainly via the Embden-Meyerhof-Parnas (EMP) pathway and the tricarboxylic acid (TCA) cycle. In general, glucose is dissimilated to pyruvate through the EMP pathway. Then pyruvate is transported to the mitochondria and converted to acetyl-CoA, which combines with oxaloacetate to form citrate. Through catalysis of aconitase, citrate is dehydrated to *cis*-aconitate that is further catalyzed to itaconate by *cis*-aconitate decarboxylase (CAD) (see Figure 1.3). In early research, Bentley and Thiessen showed that *A. terreus* NRRL 1960 utilized ^{14}C label glucose to produce IA via citrate (Bentley and Thiessen, 1957a, b). More importantly, *cis*-aconitate could be converted to IA via a crude protein extract of *A. terreus* that contains *cis*-aconitate decarboxylase (CAD) (Bentley and Thiessen, 1957c). Later, Winskill showed that citrate synthase was highly active during both the growth and production phases, whereas isocitrate dehydrogenase activity was high in the growth path but decreased to $1/8^{th}$ that value in the production phase. Furthermore, incorporation of [1-^{14}C] acetate and [2-^{14}C] acetate supports the production of IA via the TCA cycle (Winskill, 1983). Later, Bonnarme et al. confirmed that pyruvate is dissimilated into *cis*-aconitate, which is then decarboxylated to itaconate, and verified the model proposed by Bentley and Thiessen (Bonnarme et al., 1995). However, the exact metabolic pathway of itaconic acid has not been

fully completed due to two factors. As shown in Figure 1.3, the biosynthesis route seems to occur both in the cytosol and mitochondria (Jaklitsch et al., 1991). Many microorganisms contain isoforms of key enzymes involved in biosynthesis, such as aconitases (Beinert and Kennedy, 1993a; Van Der and Caspers, 2007) . Therefore, future work is needed to verify the entire pathway.

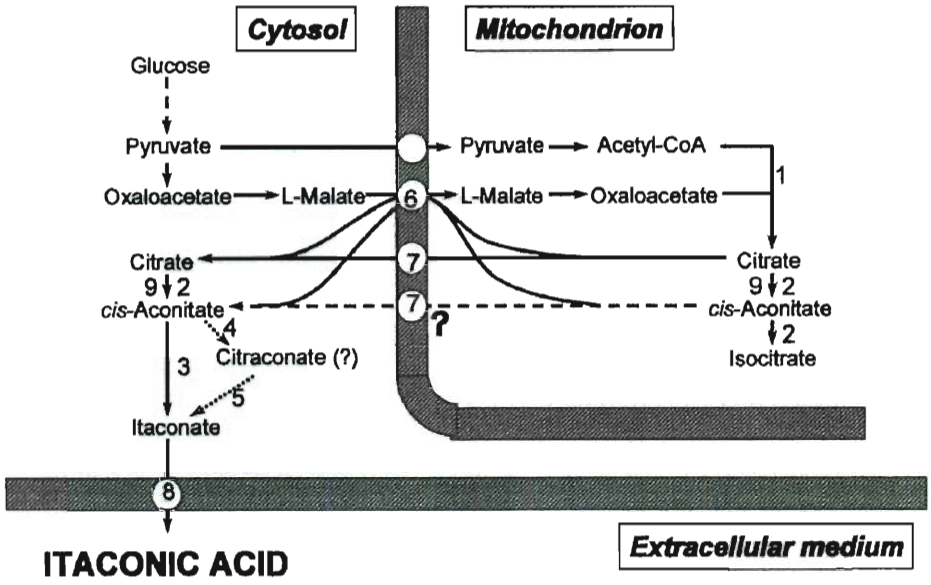

Figure 1.3 – Postulated biosynthesis route(s) for itaconic acid in *A. terreus*.
1, Citrate synthase; 2, Aconitase; 3, *cis*-aconitic acid decarboxylase (itaconate-forming); 4, *cis*-aconitic acid decarboxylase (citraconate-forming); 5, citraconate isomerase; 6, mitochondrial dicarbocylate-tricarbocylate antiporter; 7, mitochondrial tricarboxylate transporter; 8, dicarbocylate transporter; 9, 2-methylcitrate dehydratase. **(Van Der and Caspers, 2007)**

1.3.4 Characteristics of *cis*-aconitate decarboxylase (CAD)

According to Figure 1.3, two enzymes, *cis*-aconitate decarboxylase (CAD) and aconitase (Acn), are crucial for the biosynthesis of IA. Although CAD was discovered in cell lysates of *A. terreus* (Bentley and Thiessen, 1955), CAD was not isolated as homogeneous protein until 2002 (Dwiarti et al., 2002). CAD has a size of 55 kDa and shows optimal pH and temperatures of 6.2

and 37°C, respectively. This enzyme has a Km value for *cis*-aconitate of 2.45 mM at the optimal conditions. Moreover, IA production correlates with CAD activity, meaning that CAD is essential to IA production (Dwiarti et al., 2002). The *ATEG_09971* gene (*cad1*) from *A. terreus* NIH2624 was confirmed to encode CAD and the transformed *cad1* gene expressed functional protein in yeast. More importantly, a transcription assay of *cad1* showed that a high-producing strain had a higher expression level of *cad1* while itaconic acid has no apparent inhibitory effect on the transcription rate (Kanamasa et al., 2008).

1.3.5 General information about aconitases (Acn)

The other key enzyme is aconitase that catalyzes the reversible inter-conversion of citrate to isocitrate via *cis*-aconitate in the TCA cycle, where the [4Fe-4S] cluster is required for the binding of these substrates at the catalytic site (Beinert and Kennedy, 1993b). The aconitase family includes five discrete functional subgroups: (1) mitochondrial aconitase (mAcn); (2) fungal and bacterial isopropylmalate isomerases (IPMI); (3) homoaconitases; (4) iron regulatory proteins (IRP) and bacterial aconitase As (AcnA); (5) bacterial aconitase Bs (AcnB) (Gruer et al., 1997a; Williams et al., 2002). Eukaryotic mitochondrial aconitases mainly catalyze the second and third steps of the TCA cycle (Shadel, 2005). The X-ray structure of porcine heart mAcn was first determined with isocitrate bound to the [4Fe-4S] cluster (Lauble et al., 1992). Further, crystal structures of mAcn with the inhibitors *trans*-aconitate and nitrocitrate bound to the iron-sulfur cluster were reported and the combined results support the proposed mechanism of aconitase activity. As shown in Figure 1.4, citrate is dehydrated by aconitase to form *cis*-aconitate; *cis*-aconitate rotates 180° around an axis perpendicular to the double bond at the catalytic site. Next, the flipped *cis*-aconitate will be hydrated by aconitase to form isocitrate (Lauble et al., 1994).

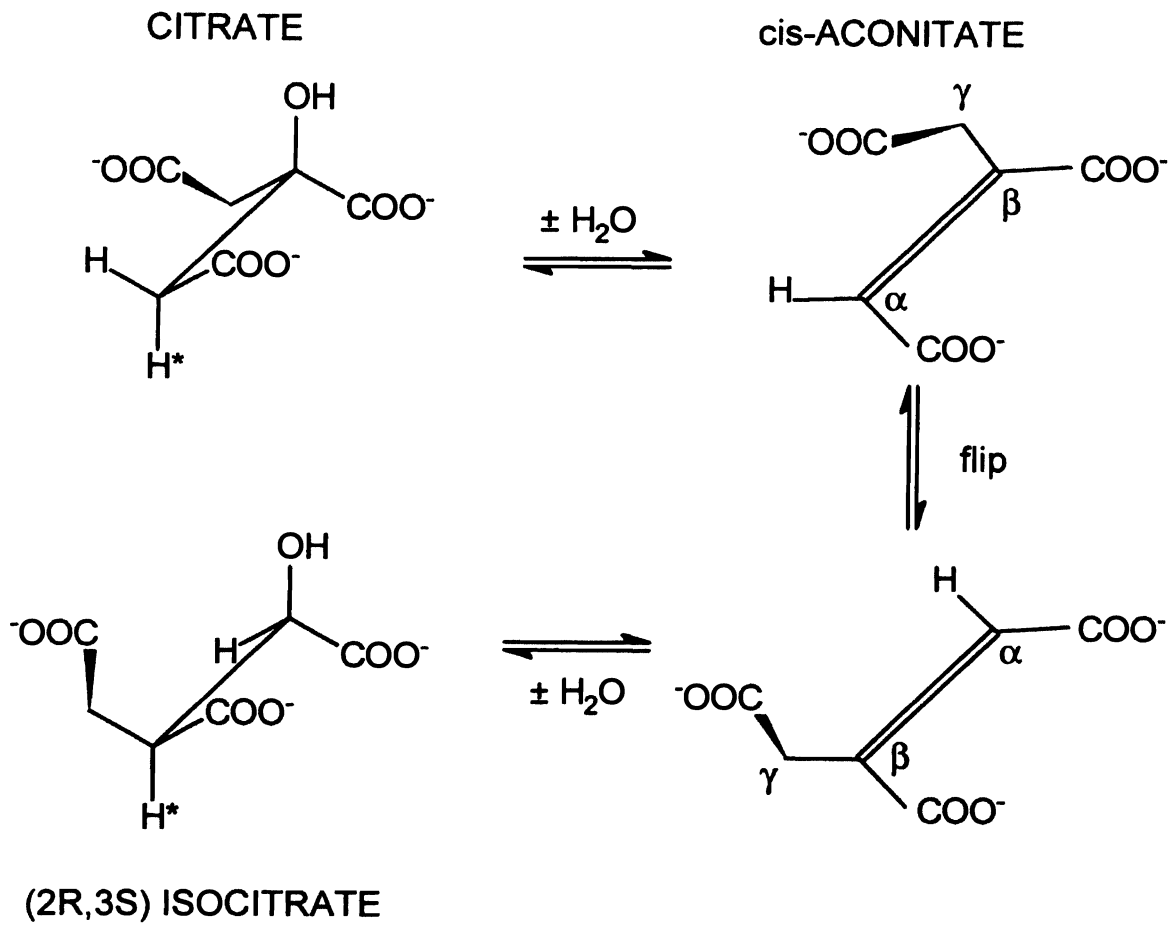

Figure 1.4 – The general mechanism of aconitase catalysis.
In general, the hydroxyl group and the proton from citrate are removed by aconitase to from *cis*-aconitate. Next, *cis*-aconitate rotates 180° around an axis perpendicular to the double bond. Next, *cis*-aconitate is further hydrated to form isocitrate. (Lauble et al., 1994)

The mAcn consists of 4 domains, where domain 4 is connected to domain 3 with a flexible linker (see Figure 1.5) (Lauble et al., 1992). Twenty amino acids were identified to be involved in the aconitase catalytic function: seven residues in domains 1, 2 and 3 are involved in substrate recognition; six in domains 1, 2 and 4 interact with the iron-sulfur cluster; seven in domains 1, 2 and 4 catalyzed the reaction (Frishman and Hentze, 1996; Gruer et al., 1997a). Site mutation analysis shows that Arg^{580} is critical in substrate binding; Asp^{100} and His^{101} eliminate the hydroxyl group from substrates; Ser^{642} functions as proton donor or acceptor (Zheng et al.,

1992). In contrast, IMPI is involved in the leucine biosynthesis pathway (Frishman and Hentze, 1996), whereas homoaconitase is found only in *Saccharomyces cerevisiae* (Gruer et al., 1997a). Depending on the conditions of iron availability and stress, IRP either regulates the translation of iron metabolism genes or functions as a cytosolic aconitase (Volz, 2008).

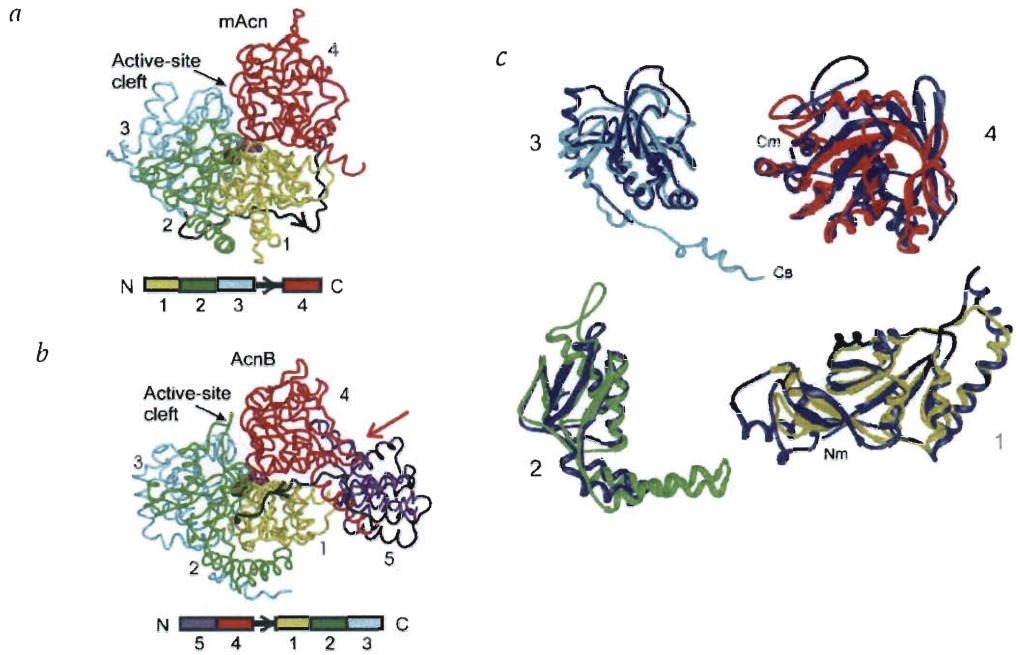

Figure 1.5 – Structure of AcnB.
(a) The structure of bovine mAcn (PDB, 1ACO). This structure contains 4 domains, where domain 4 is joined with domain 3 with a linker. *Trans*-aconitate is located in the active-site cleft. (b) The structure of AcnB. This structure contains 5 domains, where domain 4 is linked to domain 1 with a linker. An additional 5th domain is connected with domain 4. (c) Comparison of the 4 domains of mAcn and AcnB. The domains match well, but some regions of domains separate apart. Adopted from (Williams et al., 2002).

1.3.6 Aconitases in *E. coli*

Table 1 - Enzymatic activities of AcnA and AcnB

Enzyme	Substrate	Km (mM)	Substrate	Km (mM)
AcnA	Citrate	1.16	*cis*-aconitate	0.058
AcnB	Citrate	11	*cis*-aconitate	0.016

Adapted from Brenda Enzyme Database

E. coli cells possess two major distinct aconitases, AcnA and AcnB (Gruer and Guest, 1994). Both proteins require a [4Fe-4S] for their function (Jordan et al., 1999) and are highly regulated by various enzymes (Cunningham et al., 1997). Both of them can utilize citrate and *cis*-aconitate as substrates to produce *cis*-aconitate and isocitrate, respectively (Table 1) The AcnB is the major TCA cycle enzyme during exponential growth, whereas the AcnA is expressed in the stationary phase or under stress conditions (Cunningham et al., 1997; Gruer et al., 1997b). Like mAcn, AcnA has 4 domains and displays the highest identity (53%) with iron regulatory factor (IRF) (see figure 4a) (Bennett et al., 1995). In contrast, AcnB represents a unique bacterial aconitase and possesses an extra N-terminal fifth domain, which resembles a HEAT (Hungtingtin-Elongation-A subunit-TOR) domain (Williams et al., 2002). The HEAT-like domain not only facilitates the homodimerization of AcnB, but also assists in post-transcriptional regulation of gene expression (Tang et al., 2005; Williams et al., 2002). In addition, both aconitases in *E. coli* are sensitive to superoxide (Gardner and Fridovich, 1991, 1992), nitric oxide (Gardner et al., 1998; Gardner et al., 1997), and iron depletion (Varghese et al., 2003).

1.3.7 The 2-Methylcitrate dehydratase from *Shewanella oneidensis (S. oneidensis)*

Beyond the major aconitases mentioned above, a special enzyme called 2-methylcitrate dehydratase that participates in the propionic acid cycle (Brock et al., 2002; Horswill and Escalante-Semerena, 1999). As shown in Figure 1.6, with the help of accessory protein PrpF,

acnD could only convert 2-methylcitrate to 2-methylcitrate isocitrate, which is further catalyzed by AcnB to produce 2-methylisocitrate.

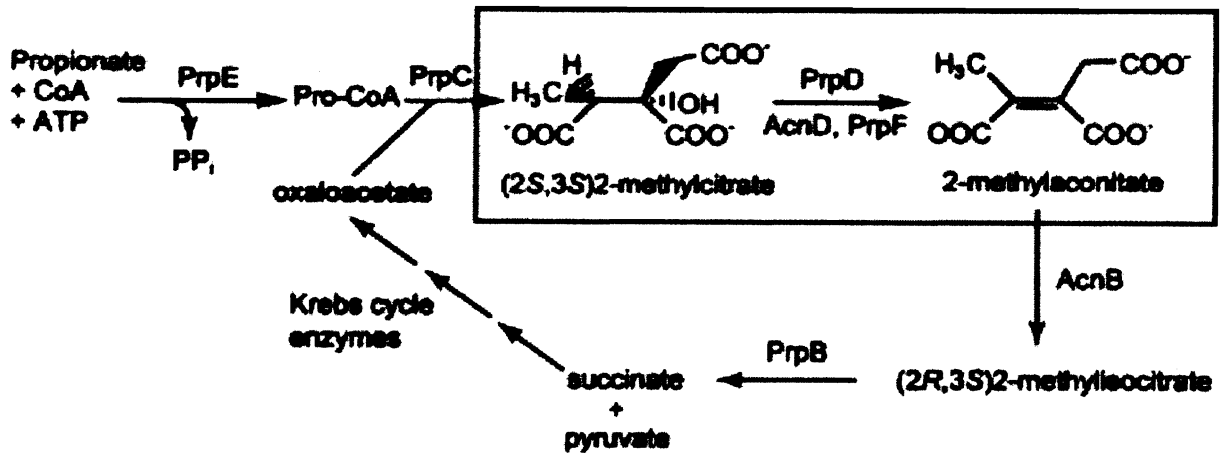

Figure 1.6 – Schematic representation of the 2-mehtylcitraic acid cycle with an emphasis on the chemical transformations catalyzed by either PrpD or AcnD/PrpF. (Garvey et al., 2007)

Substrate	AcnD	AcnA
Citrate	2.9 ± 0.5	26.5 ± 4.0
cis-Aconitate	5.0 ± 0.2	68.5 ± 7.4
Isocitrate	ND	43.4 ± 3.1
2-Methylcitrate	7.8 ± 0.4	ND
2-Methylisocitrate	ND	12.7 ± 1.4

Table 2 – Specific activity of AcnD and AcnA with different substrates (Grimek and Escalante-Semerena, 2004).
ND – No detectible activity observed under the conditions tested. Specific activities were reported in micromoles per minute per milligram of protein and calculated from the extinction coefficients of 3,600 M^{-1} cm^{-1} for the *cis*-aconitate and 4,500 M^{-1} cm^{-1} for the 2-methyl-*cis*-aconitate.

More interestingly, the AcnD from *Shewanella oneidensis (S. oneidensis)* shows no enzymatic activity with isocitrate, but can utilize citrate or *cis*-aconitate in vitro tests compared to AcnA from *E.coli* (Table 2) (Grimek and Escalante-Semerena, 2004). Furthermore, AcnD requires the accessory protein PrpF for its function (Grimek and Escalante-Semerena, 2004). X-ray structure and in vitro analysis shows that PrpF isomerizes *trans*-aconitate to *cis*-aconitate, which serves as a substrate for AcnB in the propionic acid pathway (Garvey et al., 2007). Protein

sequence alignment between AcnD and porcine heart aconitase (mAcn) shows that AcnD possesses 18 of 20 conserved active residues, whereas Gln72 and Arg580 are switched to His and Asp, respectively. Gln72 and Arg580 are crucial for substrate binding (Lauble et al., 1992); they interact with one pair of oxygen atoms in the Cγ carboxyl group of isocitrate (Lauble et al., 1994). These mutations may cause the enzyme to lose the contact with isocitrate and may explain why AcnD shows no activity with isocitrate. Future research is required to confirm this finding.

1.3.8 Debate on the existence of citrate dehydratase

To gain more knowledge about this special *A. terreus* aconitase, we choose to study the aconitase from *A. niger* as an initial alternative. *A. niger* is a well-known fungus that is used to produce citric acid commercially, another intermediate during the biosynthesis of itaconate. *A. niger* and *A. terreus* are evolutionarily closed-related and share many identities. Importantly, early publications provided us with some preliminary data on *A. niger* aconitase. Neilson reported that the citrate dehydratase ("aconitic hydratase") in *A. niger* strain 72-4 mainly performed the inter-conversion of citrate and *cis*-aconitate. (Neilson, 1955, 1956) However, La Nauze disagreed with this idea. The experimental results showed that the activities of aconitase didn't differ greatly in the reaction of citrate→*cis*-aconitate or isocitrate→*cis*-aconitate. The aconitase remained active during the entire fermentation and the concentration of ferrous ion affected the aconitase activity. (La Nauze, 1966) La Nauze's conclusions were further supported by findings of Kubicek and Rohr. They could not detect citrate dehydratase in their *A. niger*. (Kubicek and Rohr, 1985) Although the same strain of *A. niger* was used, Neilson and La Nauze used different methods to perform their research. The Kubicek group applied similar techniques as the La Nauze group, but different strains of *A. niger* were used during the research. Thus, it will be curious to see if *A. niger* has a special citrate hydratase.

1.3.9 Sequence analysis of potential aconitases from *A. terreus*

Currently, no *A. terreus* aconitases participating in the biosynthesis of IA have been reported in the databases. Beyond producing itaconic acid, a mutant strain of *A. terreus* has been patented for production of *cis*-aconitic acid (Holdom and Winskill, 1988). We suspect the *cad* gene in this strain may have become nonfunctional. Consequently, *A. terreus* accumulates the intermediate, *cis*-aconitate, without further degradation. As shown in Figure 1.7, bioinformatics analysis shows that 4 hypothetical aconitase genes are can be detected in *A. terreus* NIH2624: *ATEG_03325* (mitochondrial precursor) and *ATEG_08913* (cytosolic precursor) under non-itaconic acid producing conditions; *ATEG_02937* (mitochondrial precursor) and *ATEG_05743* (cytosolic precursor) under itaconic acid producing conditions.

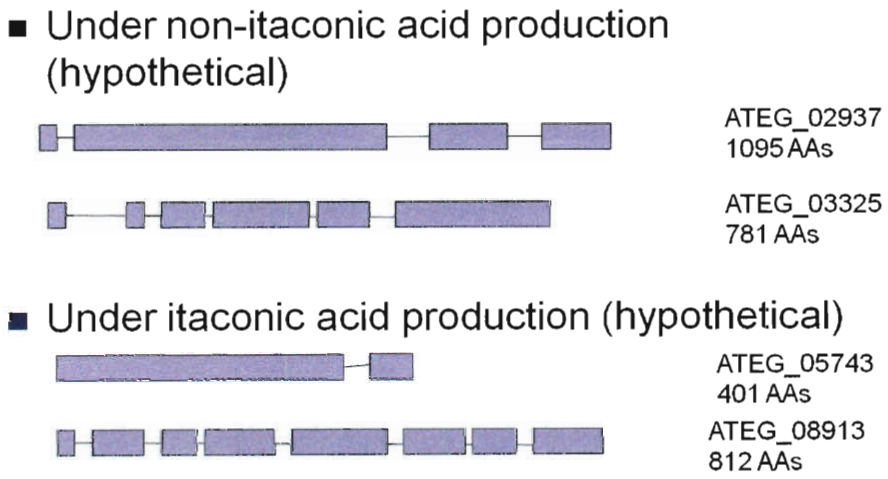

Figure 1.7 – Four candidate aconitase genes from *Aspergillus terreus* NIH2624.
The genes ATEG_02937 and ATEG_03325 are expected to express under the condition of non-itaconic acid production; the genes ATEG_05743 and ATEG_08913 are expected to express under the conditions of itaconic acid production.

Protein sequence alignment between *S. oneidensis* AcnD and *A. terreus* NIH2624 genome reveals that *ATEG_03325* encoding for XP_001212503 shows the best identity with AcnD (188 hits) and reserved all the residues at the active site (Frishman and Hentze, 1996). On the other hand, *ATEG_02937* encoding for XP_001212115 is the second most identical (166) to AcnD; it conserved 18 residues at its active residues while Arg^{580} and Ser^{643} are changed to Lys and Ala, respectively. Arg^{580} is thought to participate in the 180° flip of *cis*-aconitate in the active site, whereas Ser^{643} interacts with the Cβ carboxyl group of isocitrate (Lauble et al., 1992). These mutations may cause the enzyme to only dehydrate citrate and allow the *A. terreus* to accumulate *cis*-aconitate without consuming it. Therefore, cloning *ATEG_02937* is of interest to pursue in the research.

CHAPTER 2. Materials and Methods

This Chapter describes the materials and methods used to perform the research presented in this work.

2.1 Strains and plasmids

The strains and plasmids utilized during the research are listed in Table 2 and 3.

Table 3 - List of strains and plasmids used in this research

Strain	Significant Genotype	References
GNB 11338	*ΔacnB736::kan*	(Baba et al, 2006)
GNB 11339	*ΔacnA785::kan*	(Baba et al, 2006)
GNB 10257	Wild type, = MG1655	This Study
TOP 10	rpsL(Str^R)	Invitrogen
GNB 11315	Chromosomal P_{ara}-*groEL/S*	(Guisbert et al., 2004)
GNB 11321	Chromosomal $P_{A1/lacO-1}$-*dnaK/J-lacI^q*	(Guisbert et al., 2004)
BL21	lacI lacUV5-T7 gene	Promega
XL1-Blue	*Tn*10 *(Tet^r)*	Stratagene

Plasmid	Genotype	References
pTrc99a	Cloning vector, Ap^R	Pharmacia
pTrcHis	Cloning vector, Ap^R	Invitrogen
pDHC29	Cloning vector, Cm^R	(Philips et al., 2000)
pET32a	Cloning vector, Ap^R	EMD
pThioHisB	Cloning vector, Ap^R	Invitrogen
pPRP140	Cloning vector, Ap^R	(Grimek and Escalante-Semerena, 2004)
pTrc99a-*cad*	Synthetic *cad* gene inserted into pTrc99a vector	This Study

Table 4 - List of Fungi in this project

Strain	Reference
Aspergillus niger DSM 872	German Collection of Microorganisms and Cell Cultures
Aspergillu terreus NIH2624	Fungal Genetic Stock Center

2.2 Media

2.2.1 LB medium and *Aspergillus* medium

Luria Bertani (LB) broth medium was prepared by mixing 10 g/L tryptone, 5 g/L yeast extract, and 10 g/L NaCl in distilled water. LB medium was supplemented with carbon sources such as glucose, *cis*-aconitate, and citrate in various concentrations specific to the experiments. The LB medium was autoclaved and the carbon sources were filter-sterilized and added afterwards.

Antibiotics were added to the final concentrations of 100 ng/mL ampicillin, 50 ng/mL kanamycin, and 35 ng/mL chloramphenicol to select the strains and plasmids with antibiotic resistance. Isopropyl-β-thiogalactopyranoside (IPTG) was added to a final concentration of 1 mM to induce genes under control of the pTrc promoter. Arabinose was added to a final concentration of 500 ng/μL and to induce genes under control of the pBAD promoter.

Aspergillus complete medium (CM) was prepared by following the protocol from Dr. May's Lab (M.D. Anderson Cancer Center, Houston, TX). In this protocol, sodium nitrate is replaced by ammonium tartrate in the protocol. (See Appendix)

2.2.2 Storage Medium

2.2.2.1 Glycerol stocks

Glycerol stocks were prepared to store the *E. coli* strains for long term storage. These stocks consisted of 500 μL of filter-sterilized 40% glycerol and 500 μL of overnight cultures. After mixing the cells by vortexing, the stock was left at room temperature for 1 hr, and then stored in the block at -80 °C. For *Aspergillus* species, the glycerol stocks consist of 500 μL of

filter-sterilized 10% glycerol and 500 μL of collected spores. After mixing the spores by vortexing, the stock was quickly frozen by liquid nitrogen, and then stored in the block at -80 °C.

2.2.2.2 Agar plates

Agar plates were prepared by mixing LB or CM medium with 15 g/L technical agar. After autoclaving, the agar mixture was cooled to around 55 °C before addition of the proper antibiotic, IPTG, arabinose, and so on whenever required. Cells were selected on the plates and stored in refrigerator for a short period of time.

2.3 Cell Cultivation

2.3.1 Overnight aerobic tubes

A single colony of *E. coli* from the LB agar plate or the glycerol stock was inoculated in 5 mL LB medium with appropriate antibiotic. The cultures were grown in the shaker at 30 or 37 °C at 250 rpm.

2.3.2 Collect the spores from *Aspergillus* species

A single colony of *Aspergillus* species from the complete medium plate was spread as a lawn on a new complete medium plate. The plate was incubated at 30 °C for 2 days. The spores were collected with 5 mL Tween 20, washed twice with sterilized water, and filtered through miracloth with 3 mL water. The number of spores was counted in hemocytometer under the microscope.

2.3.3 Aerobic Shake Flask

The aerobic shake flask experiments of *E. coli* were performed in 250 mL shake flasks containing 50 mL LB medium. The medium was supplemented with the appropriate amounts of carbon sources and antibiotics as needed. The overnight cultures were inoculated with a final OD = 0.05 and grown at 25, 30 or 37 °C with 250 rpm shaking. After the OD reaches 0.4 – 0.6, the cultures were induced with 1mM IPTG or 500 ng/μL arabinose as required. Samples were collected at various time points dependent on the experiments.

The aerobic shake flask experiments of *Aspergillus* species were performed in 250 mL shake flasks containing 50 mL complete medium with ammonium tartrate. The cultures were initiated with a number of spores equal to 1.0×10^6 /mL. They were grown at 37 °C with 250 rpm. Mycelia were collected at various time points dependent on the experiments. The collected mycelia were filtered through miracloth and freeze-dried overnight for future use.

2.4 Analytical Techniques

2.4.1 Cell Density Determination (OD)

Cell Density (OD) was measured at 600 nm in a Spectronic 1001 spectrophotometer (Baush & Lomb). The overnight cultures were diluted to the linear range (reading between 0.1-0.6 OD_{600}) with sterilized water in 1/10 dilution. The actual cell density was calculated based on the reading and dilution ratio. The ODs from the samples of aerobic shaking flasks were measured directly without any dilution.

2.4.2 Extracellular metabolites analysis - HPLC

To quantify excreted metabolites from the fermentation broth, 1 mL of culture was centrifuged at 13,000 rpm for 3 minutes. The supernatant was filtered through a 0.2 um PVDF membrane syringe filter and stored frozen at -20 °C until analysis. The extracellular metabolites, including the carbon sources, were quantified using a HPLC system (Shimadzu-10A systems, Shimadzu, Columbia, MD). This HPLC system was connected with a cation-exchange column (HPX-87H, BioRad Labs, Hercules, CA), a differential refractive index (RI) detector (Water 2410, Waters, Milford, MA) and an ultraviolet detector (UV) (Shimadzu SPD-10A). A 2.5 mM H_2SO_4 solution flowed through the system at 0.5 ml/min as a mobile phase, while the column was operated at 55 °C. Calibration curves of standard metabolites were established for the interested metabolites in both RI detector and UV detector. Glucose, succinate, lactate, formate, acetate, and ethanol were detected in the RI detector and pyruvate, citrate, isocitrate, *cis*-aconitate, trans-aconitate, and itaconate were detected in the UV detector.

2.4.3 Enzyme Assays of CAD

2.4.3.1 Crude Extract

Volumes of 5, 10, or 50 mL of the *E. coli* cell cultures were harvested by centrifugation at 7000 rpm at 4 °C for 5 min. The supernatants were stored for HPLC analysis and the cell pellet was resuspended in the following buffer: 2.5 mM NaH_2PO_4 pH 6.5 containing 1mM DTT, 0.1 mM EDTA, and 1 mM PMSF. The cell extracts were prepared immediately by sonicating the cell on ice at 50 or 75 W for 3 min with 30 sec pulse ON and OFF (Sonicator: Heat System Ultrasonics, Inc Model W-255). The sonicated cells were centrifuged at 10,000 rpm at 4 °C for 10-15 min to remove cell debris. The resulting crude extracts were immediately analyzed or kept

at 4 °C and analyzed within the next 12 hours. Total protein concentration in cell extracts was analyzed with Bradford reaction (Biorad) using bovine serum albumin as standard.

The mycelia of *Aspergillus* species were ground with glass beads for 3-5 minutes. The ground power was re-suspended in the following buffer: 20 mM Hepes pH8.0 containing 20% glycerol, 0.1 M KCl, 0.2 mM EDTA, 0.5 mM PMSF, and 0.5 mM DTT. The mixture was transferred on the ice for 15 minutes and agitated to completely suspend the protein in the buffer. Next, the mixture was centrifuged at 12,000 x g for 10 min at 4 °C. The supernatant was further centrifuged at 24,000 rpm for 35 min at 4 °C. Total protein concentration in cell extracts was analyzed with Bradford reaction (Biorad) using bovine serum albumin as standard.

2.4.3.2 CAD enzyme assay

Cis-aconitate decarboxylase (CAD) activity was measured using a modification of a previously described method (Dwiarti et al., 2002; Kanamasa et al., 2008). CAD catalyzes *cis*-aconitate to itaconate with the release of CO_2. *Cis*-aconitate and itaconate were detected by 210 nm UV detector at 9.8 min and 15.3 min, respectively. The amount of itaconate produced in the assay was used to determine the activity of CAD.

2.4.3.3 Aconitase assay

The aconitases from the experiments were activated for 30 min by Tris buffer pH 7.4 including 40 mM Tris-HCl, 5 mM DTT, 1 mM $(NH_4)_2Fe(SO_4)_2$, and 1 mM Na_2S. (Jordan et al., 1999; Tsuchiya et al., 2009) The activated aconitase was reacted with 10 mM of citrate or isocitrate in 50 mM Tris pH 7.4 buffers containing 1M NaCl, 5 mM DTT, and 5 mM PMSF. The reaction was conducted at 37 °C for 30 min and quenched with 100 µL of concentrated hydrochloric acid. The reaction mixture was analyzed in the HPLC. By analysis with the 210 nm

UV detector, *cis*-aconitate appeared at 9.8 min in the spectra, whereas citrate and isocitrate overlapped at 10.3 min. The amount of *cis*-aconitate produced in the assay was used to determine the activity of aconitase.(La Nauze, 1966; Tsuchiya et al., 2009)

2.5 Genetic Manipulation

2.5.1 Chromosomal DNA Purification and Plasmid Isolation

Chromosomal DNA of *E. coli* was extracted using Puregene® a genomic DNA purification kit from Gentra Systems (Gentra Systems, Minneapolis, MN). The chromosome DNA was used as a template to examine the genes of interest. The chromosomal DNA from *Aspergilleus terreus* was obtained using yeast DNA extracting kit. The chromosomal DNA from the fungi was used to amplify the genes of interest. Plasmids were purified using the GenElute Plasmid Mini-Prep kit from Sigma Aldrich by following the instructions suggested by the manufacturer.

PCR products were purified using the QIAquick PCR Purification Kit (QIAGEN, Valencia, CA) by using the manufacturer's protocol. DNA products including digested fragments and PCR products in agarose gels were purified using the QIAEX II Gel Extraction Kit (QIAGEN, Valencia, CA) by following the attached protocol.

2.5.2 DNA Digestion and Ligation

Plasmid and DNA were digested by restriction enzymes obtained from New England Biolabs (Beverly, MA), Promega (Madison, WI), and Fisher (Pittsburgh, PA) by following the protocol suggested by the manufacturer. Ligation reactions were performed using the T4 DNA Ligation Kit from Sigma as described by the protocol.

2.5.3 Agarose Gel Electrophoresis

Agarose gel electrophoresis was used to separate and verify the sizes of DNA fragments from either PCR products or plasmid digests. The gel was prepared by mixing 1 gram of agarose with 100 mL of TAE buffer (40 mM Tris-acetate, 2 mM EDTA at pH8). 1 μg/mL of ethidium bromide or SYBR Safe DNA gel stain (Invitrogen) was added into the gel after cooling down to 60 °C. The gel was solidified in the electrophoresis chamber and immersed in the TAE buffer during the electrophoresis. Samples and DNA ladders were then loaded into the gel sample wells, respectively. The DNA fragments were separated based on the size after applying 100 constant volts across the gel for 1 hour. The DNA bands were visualized under the UV light, due to the fluorescence emitted by the added DNA dye that intercalates between the bases of DNA.

2.5.4 PCR

Polymerase chain reaction (PCR) was done to amplify the number of copies of a particular gene for various goals, such as to confirm insertion of a new gene, to clone an interested gene, or to verify correct mutations. Primers were designed for PCR reactions following standard primer design procedures. The website http://www.idtdna.com provides useful tools to design the primers. Primers were designed in the idtdna website and purchased from Sigma Aldrich (Woodland, TX).

PCR was performed using an Eppendorf vapor protect PCR machine (Hamburg, Germany). The Phusion High-Fidelity PCR Kit from Finnzymes and the MasterTaq Kit from Eppendorf (Hamburg, Germany) were utilized to clone the genes by following the kit manual.

2.5.5 Cell Transformation

The chemical cell transformation was mainly employed in this study. Chemical competent cells were prepared by following RbCl Transformation Procedure for Improved Efficiency (NEB Transcript, April 1994). During the transformation, the host cells were mixed with 0.1 μg of plasmid DNA or 5-10 μL of minipreped plasmid DNA to 100 μL of the competent cells. The mixture was placed on ice for 15-30 min. Then the cells were heat-shocked at 42°C for 20-30 seconds. Immediately, the cells were transferred to ice and sit on ice for 5 min. Next, 250 μL of SOC medium was added into the cells. The cells were incubated at 37 °C at 250 rpm for 30-45 min to allow the expression of the antibiotic resistance genes. The transformed cells were selected on agar plates with appropriate antibiotic. The plates were incubated at 37°C overnight.

2.5.6 Gene Cloning and Expression

In general, the interested genes were amplified by PCR or restriction digested by certain enzymes. Next, the genes were ligated to vectors at the restriction sites. The ligation mixture was transformed into the prepared cloning host cells and the cells bearing the possible correct plasmid were selected on the selection plates, using antibiotic and X-gal containing plates with IPTG as screens for the desired phenotype. X-gal stock is prepared at 20 mg/mL in dimethylformamide. Additionally, PCR products can also been ligated directly to the certain vectors, such as pTrcHis vector (Invitrogen).

CHAPTER 3. Expression of *cad* gene in various vectors in E. coli

3.1 CAD protein expressed from pTrc99a-*cad* plasmid is soluble and functional in the cytoplasm.

The main purpose of this experiment is to determine whether the CAD protein can be expressed and functional in the cytoplasm. Based on published *cad* gene sequence (Kanamasa et al., 2008), the synthetic *cad* gene was ordered and inserted into the pTrc99a vector. This plasmid was transformed into *E. coli* strains with either *acnA* or *acnB* mutation or wild type, individually. As experimental controls, the host plasmid pTrc99a without the *cad* gene was also transformed into the same three *E. coli* strains. The overnight cultures of these strains with either pTrc99a-*cad* or pTrc99a plasmid were inoculated in new flasks containing 50 mL LB medium with 50 mM glucose. After the induction of gene expression from the plasmid for 4 hours with 1 mM IPTG, the expression of CAD in the cell lysate was analyzed using the CAD enzyme assay (Dwiarti et al., 2002). The production of IA from the supernatant was also examined by High Performance Liquid Chromatography (HPLC). The concentration of IA produced from both the assay and the supernatant of cell cultures was determined by comparison with a standard curve of IA run on the HPLC.

As shown in Figure 3.1, by analysis using the 210 nm UV detector, *cis*-aconitic acid (Sigma) displays a peak at 8.717 minutes, while itaconic acid (Sigma) is detected at 15.437 minutes. Citric acid and isocitric acid (Sigma) overlap each other at 9.973 minutes in the spectrum. RID detector is not sensitive to trace the amounts of metabolites listed above.

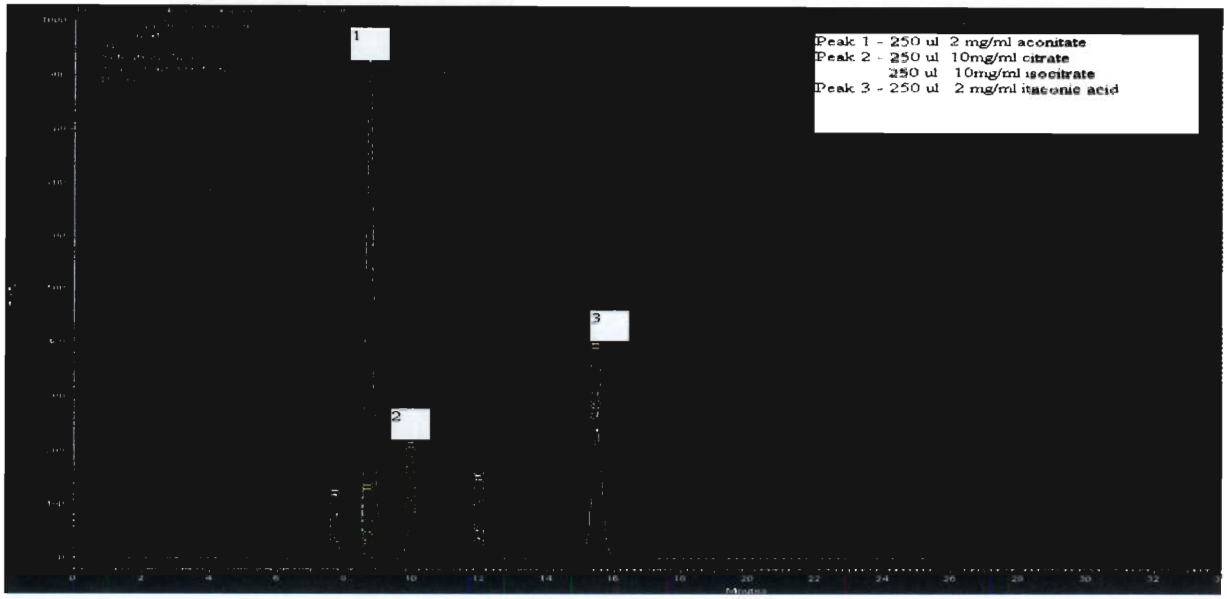

Figure 3.1 – HPLC spectrum of standard organic acids under 210 nm UV detector. Peak 1 - 250µL 2mg/ml aconitic acid; Peak 2 - overlap of 250µL 10mg/ml citric acid and 250µL 10mg/ml isocitric acid; Peak 3 - 250µL 2mg/ml itaconic acid.

In the spectrum Figure 3.2-I, *cis*-aconitic acid existed in excess as indicated by the large peak at 8.947 minutes. Importantly, a small peak at 15.443 minutes should show the production of itaconic acid, which was not found in either the positive or negative controls (Figure 3.2-II & III). The biological control was *E. coli* strain bearing pTrc99a vector without the *cad* gene, while the negative control is just the reagents for the CAD enzyme assay without the enzyme. These results indicate the *cad* gene was expressed under the induction of IPTG and CAD protein is soluble in the cytoplasm. More importantly, these results suggest that CAD protein is functional to catalyze the decarboxylation of *cis*-aconitate during the reaction. Meanwhile, a small level of IA (0.263 mM or 34.19 mg/L) was detected in the supernatant from the strain bearing *cad* gene relative to the control, as indicated by the yellow arrow in the spectra (Figure 3.3). This result

further confirms the activity of CAD. But the production rate of IA is so small that a higher expression rate of CAD with better activity was highly recommended.

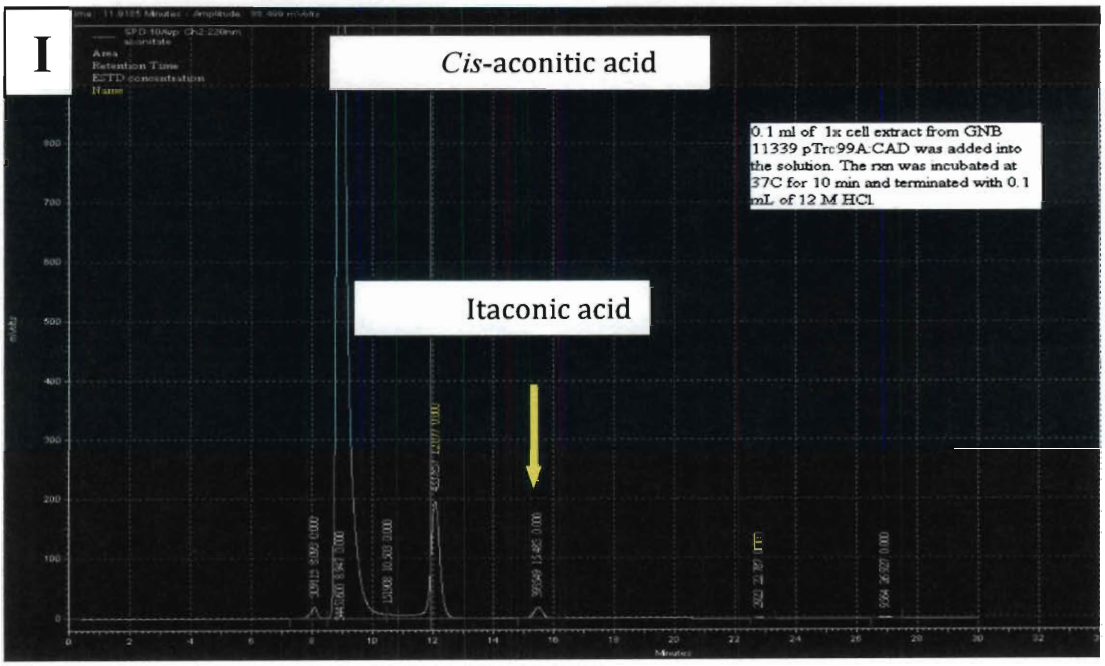

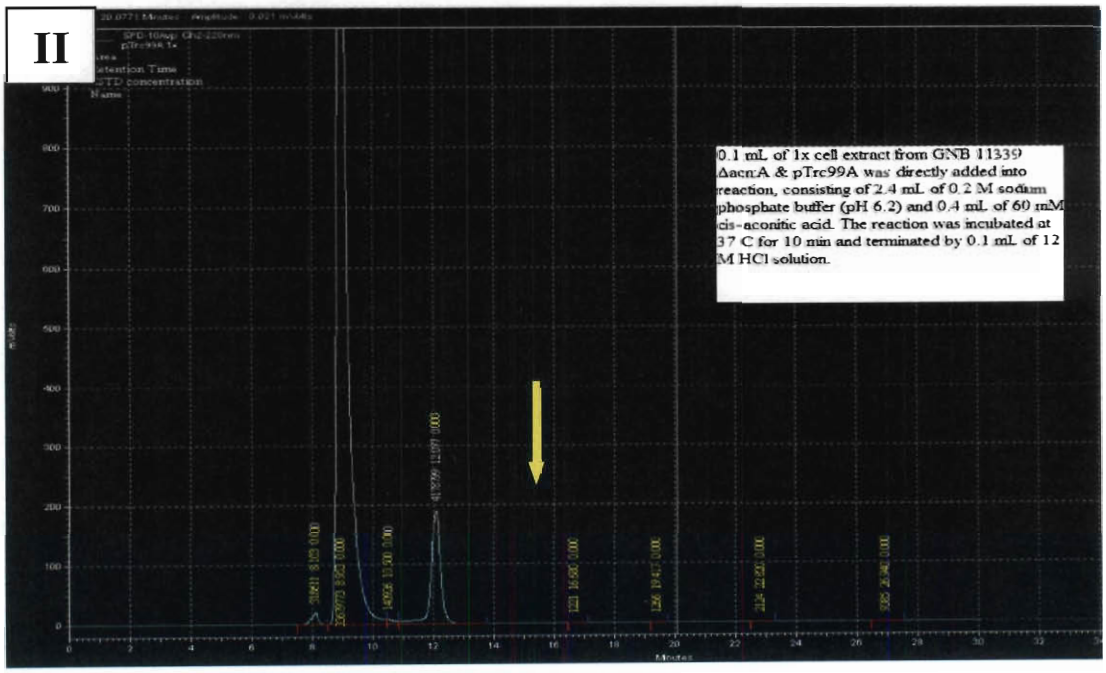

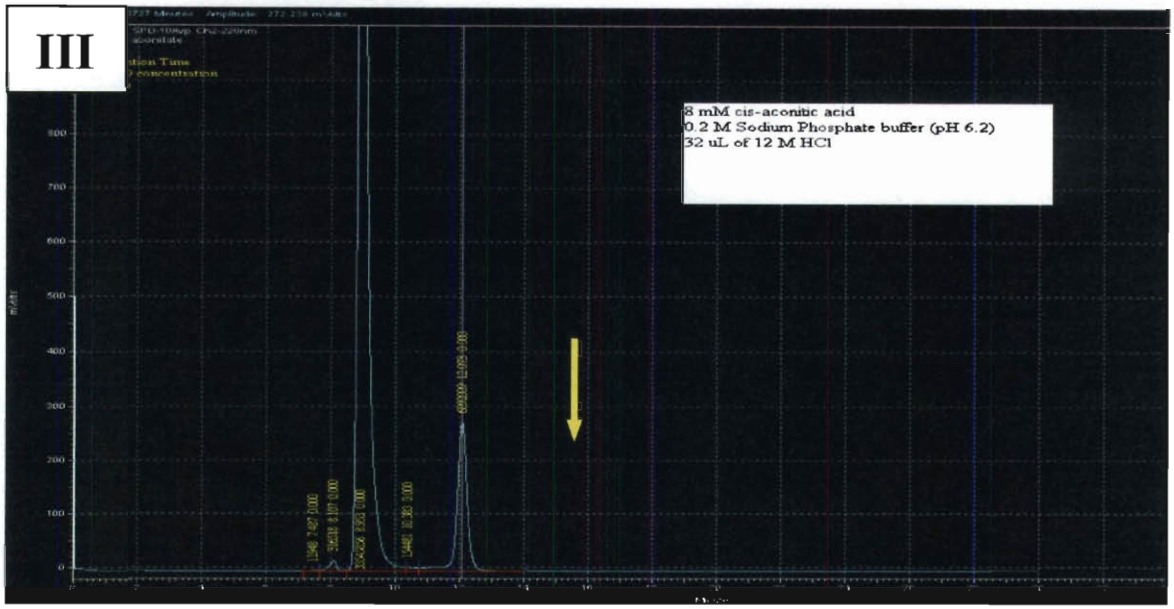

Figure 3.2 - Comparison of HPLC profiles from *cis*-aconitic acid assays.
(**I**) - 1x crude protein extract from GNB 11339 *ΔacnA::Km*^{R} pTrc99A:*cad*; (**II**) – 1x crude protein extract from GNB 11339 *ΔacnA::Km*^{R} pTrc99A; (**III**) – reagents for *cis*-aconitic acid assays. Yellow arrow indicates the retention time for IA in HPLC under 210 nm UV detector.

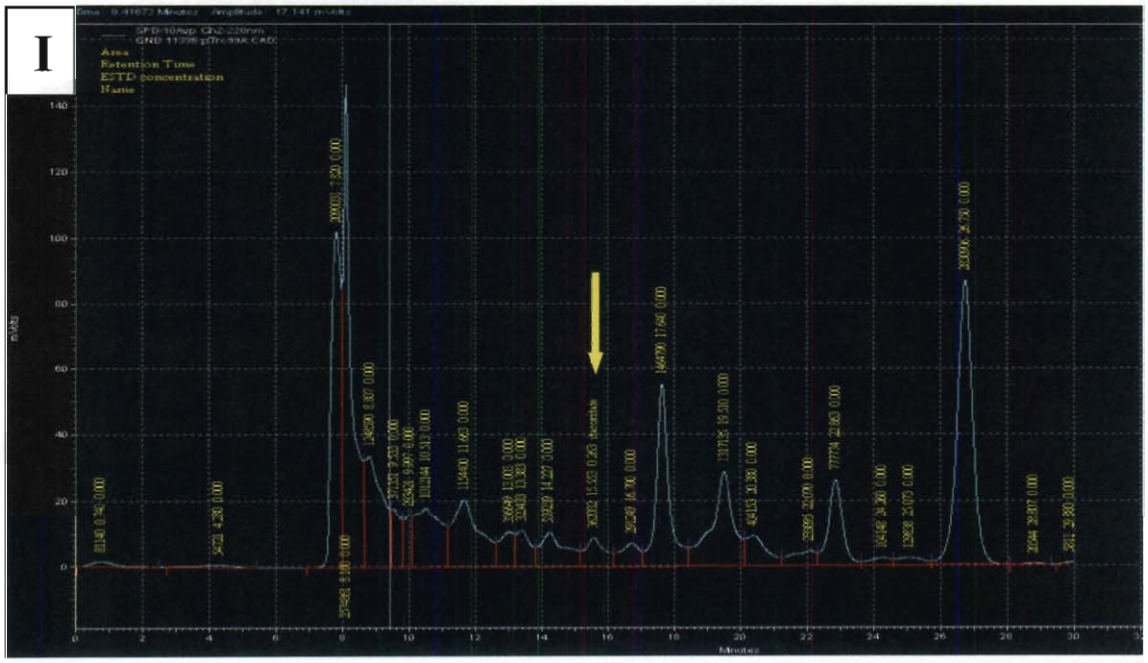

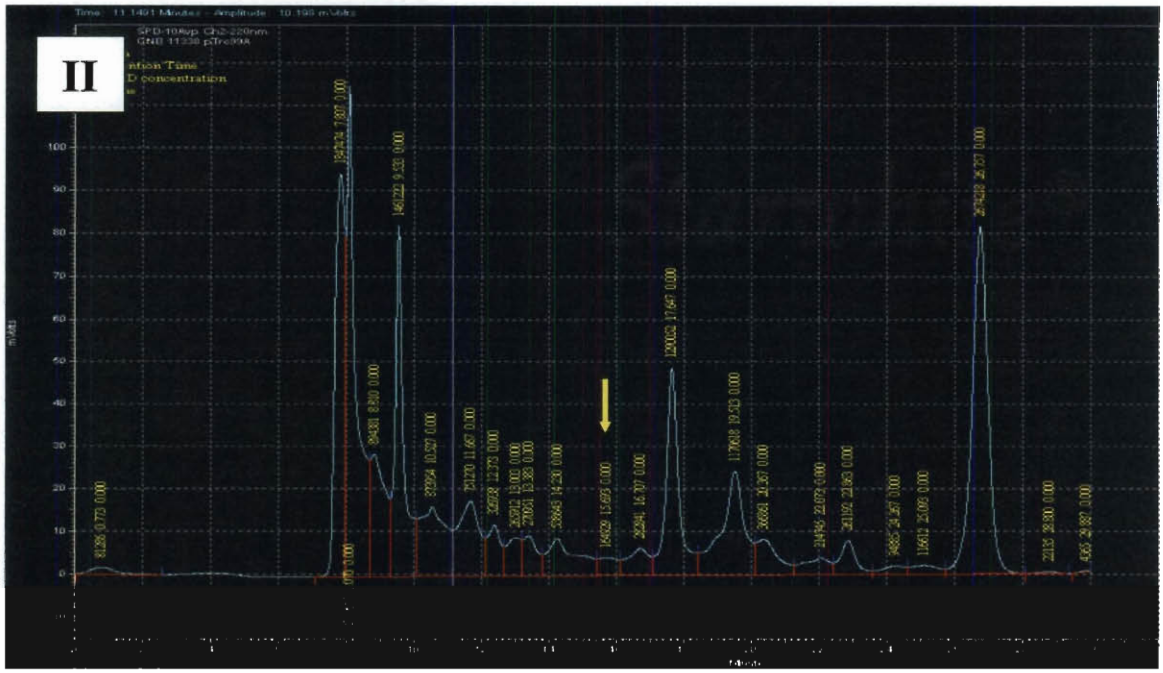

Figure 3.3 - Comparision of the contents of supernatants in HPLC after 1 day incubation for GNB 11339 ΔacnA:KMR pTrc99A:*cad* (I) and the control GNB 11339 ΔacnA:KMR pTrc99A (II).
The supernatants of cell cultures after 1 day incubation were analyzed by HPLC. Yellow arrow indicates the retention time for IA in HPLC.

3.2 CAD protein expressed from pTrcHis-*cad* vector was functional and visualized through Western Blot.

The main goal of constructing pTrcHis-*cad* plasmid is to purify the CAD protein with His-tag and to further characterize the functions and expressions level of the CAD protein. I inserted the *cad* gene into pTrcHis vector (Invitrogen) and verified the construct by restriction digest and sequencing (See Figure 3.4). With the induction of 1mM IPTG, the expression of *cad* gene was analyzed by a CAD enzyme assay in vitro. The CAD activity in the cell crude was identified by the appearance of itaconate in HPLC. The crude protein was further purified through QIAGEN Ni-NTA mini-column (QIAGEN) with centrifugation. The purified protein

was immune-precipitated by primary anti-His antibodies and detected with a secondary antibody in a Western Blot. As shown in Figure 3.5, without induction of IPTG, no strong bands were visualized in the lanes of the eluates, which were collected from each step of Ni-NTA mini-column purification using GNB11339 pTrcHis-*cad* cell crude lysate. In contrast, in extracts made form cells with induction of IPTG, a strong band from 1st eluate of GNB11339 pTrcHis-*cad* was visualized on the membrane. This band was expected to be the protein, $(His)_6$-CAD, which should have a size of 59kDa based on the published data. (Dwiarti et al., 2002; Kanamasa et al., 2008) Additionally, the 1st eluate from the induced GNB11339 pTrcHis-*cad* strain also displayed some activity in the CAD enzyme assay. However, the low resolution of this band may indicate that the amount of CAD protein in the cell crude is relatively low. Lower temperature and longer incubation time have been suggested to increase the expression and improve folding of $(His)_6$-CAD protein.

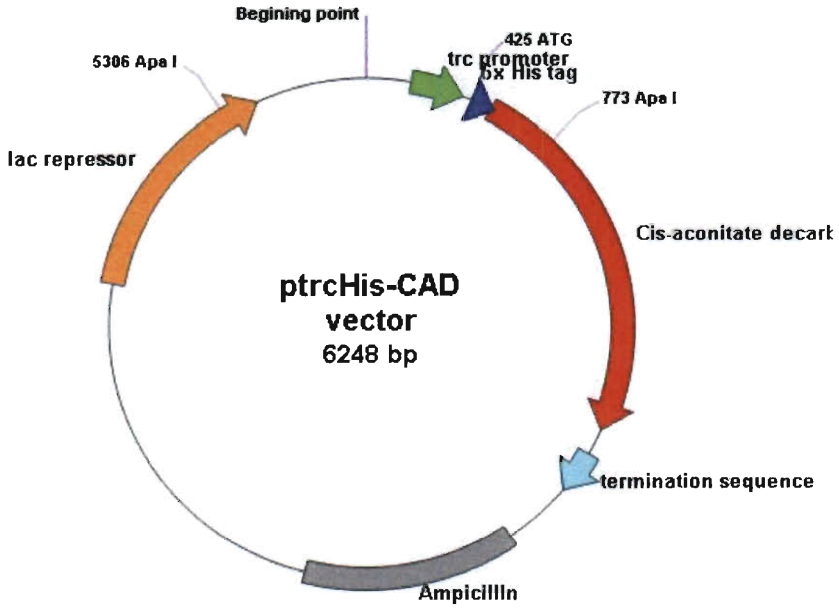

Figure 3.4 – Plasmid map of pTrcHis-*cad*.

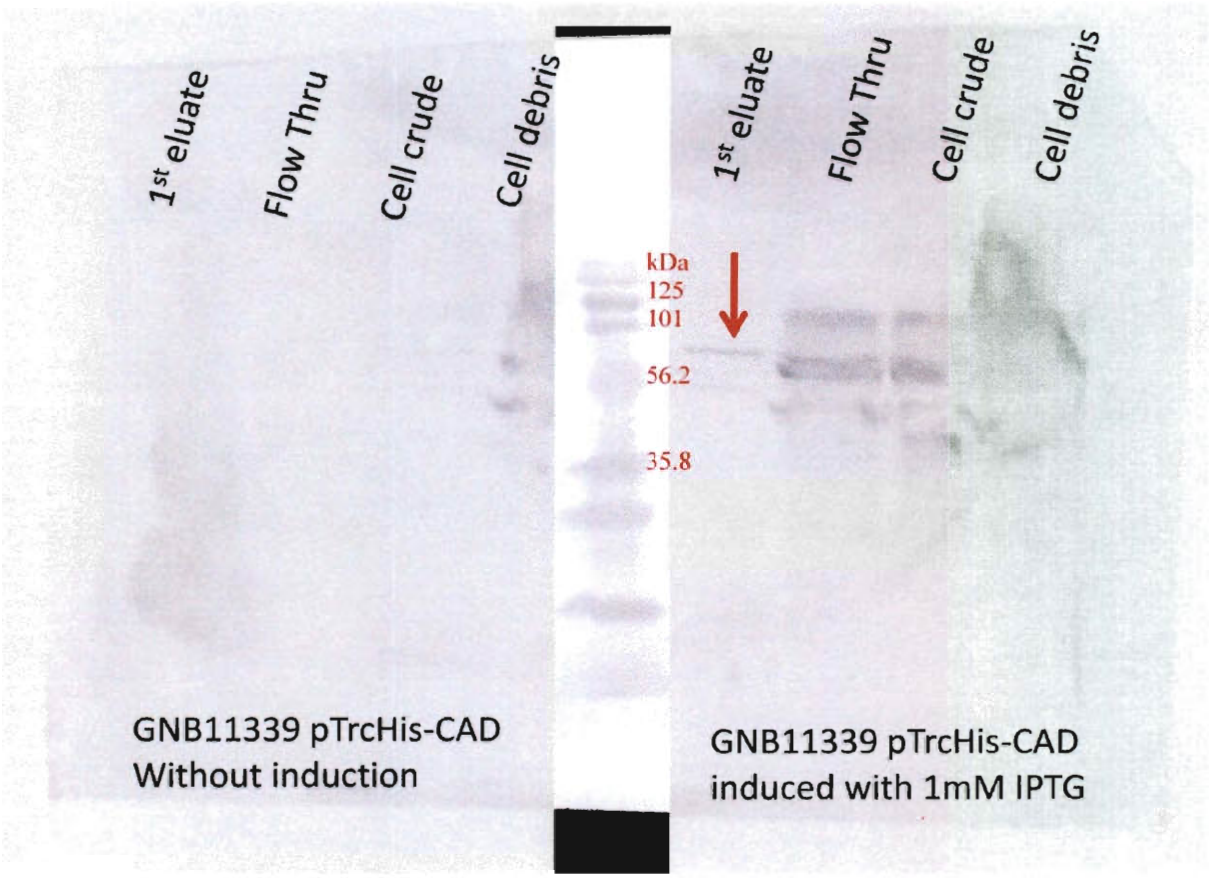

Figure 3.5 – Western blot of eluates from GNB11339 pTrcHis-*cad* with & without induction of 1mM IPTG during Ni-NTA mini-column purification.
After sonication, cell crude extract was separated from cell debris by centrifugation. Cell crude extract was subjected to Ni-NTA column using a centrifugation protocol. $(His)_6$-CAD attached to the Ni-NTA column; the rest of the cell crude extract was called flow through (flow thru) and collected. After washing the column twice to remove the contaminants, $(His)_6$-CAD was eluted by eluting buffer containing a high concentration of imidazole. The first collection was 1st eluate.

3.3 Expression of *cad* gene in other high-copy plasmids was not successful.

The main goal of building the following plasmids is to further enhance the amount of CAD protein in the expression and characterize the CAD enzymatic activity. The *cad* gene was also cloned into various vectors: pDHC29, pET-32a, and pThioHisB. Each construct was confirmed by PCR and sequencing. The purpose of constructing pDHC29-*cad* plasmid (Figure

3.6) was to over-express *cad* gene in a chloramphenicol resistant plasmid, which is highly compatible with other high copy number plasmids (Phillips et al., 2000). Unfortunately, no activity of CAD from pDHC29-*cad* plasmid was shown in the enzymatic assays. To over-express and characterize CAD protein, I attempted to insert *cad* gene into pET-32a vector (Figure 3.7). No significant activity of CAD was detected in the enzymatic assay of cell extracts made from the induced cells, either. Meanwhile, only small amount of CAD activity was detected from cells bearing the pThioHisB-*cad* plasmid (Figure 3.8). Several reasons may contribute to low activity or no function of CAD. First of all, in these constructs, a long extra protein tail from each vector has usually been inserted in front of actual CAD protein sequence. This long tail may affect the proper folding of the protein, causing its malfunction. Secondly, growth conditions may not be proper for proper folding. Although I tried to grow the cells at lower temperatures, such as 30°C and 25°C, no significant improvement of CAD activity was observed in the enzymatic assay. Thirdly, my colleagues mentioned that since CAD protein originated from fungus, over-expression of the gene in high copy plasmids may lead to aggregation of the protein. That may explain why no significant activity was detected in the enzymatic assay. Therefore, future work will be necessary to solve these problems.

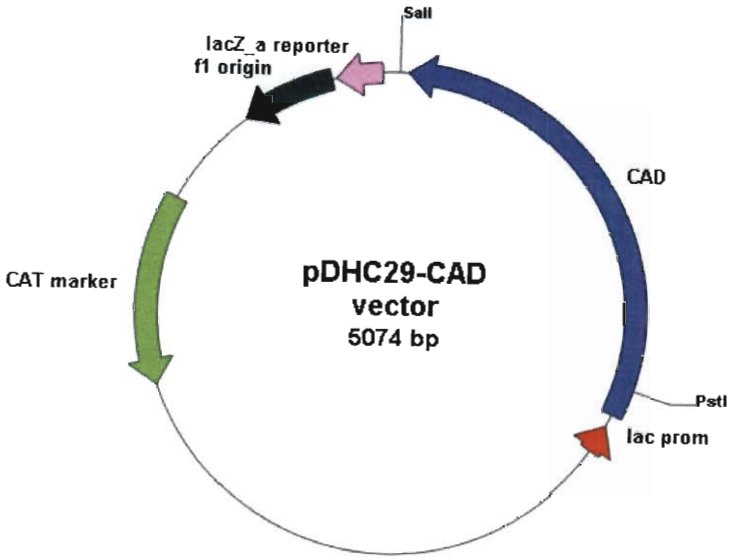

Figure 3.6 – Plasmid map of pDHC29-*cad*
The *cad* gene was inserted into pDHC29 vector at PstI and SalI sites.

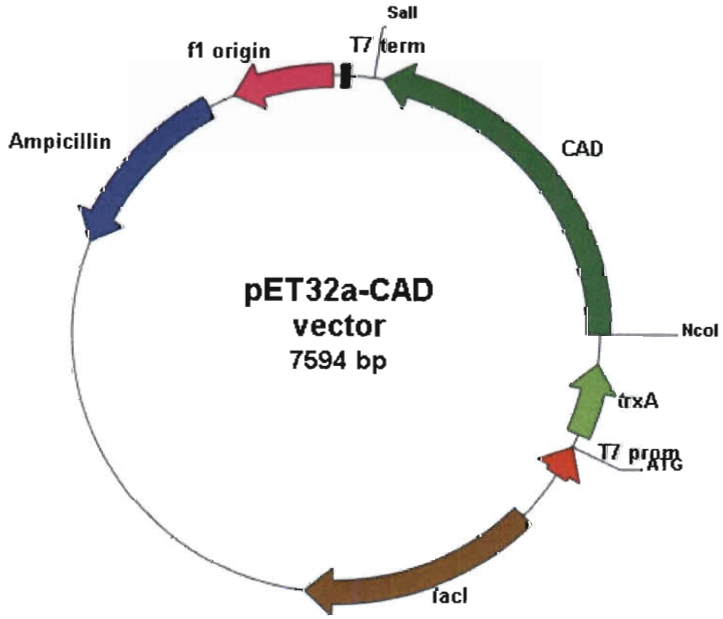

Figure 3.7 – Plasmid map of pET-32a-*cad*
The *cad* gene was inserted into pET-32a vector at NcoI and SalI sites.

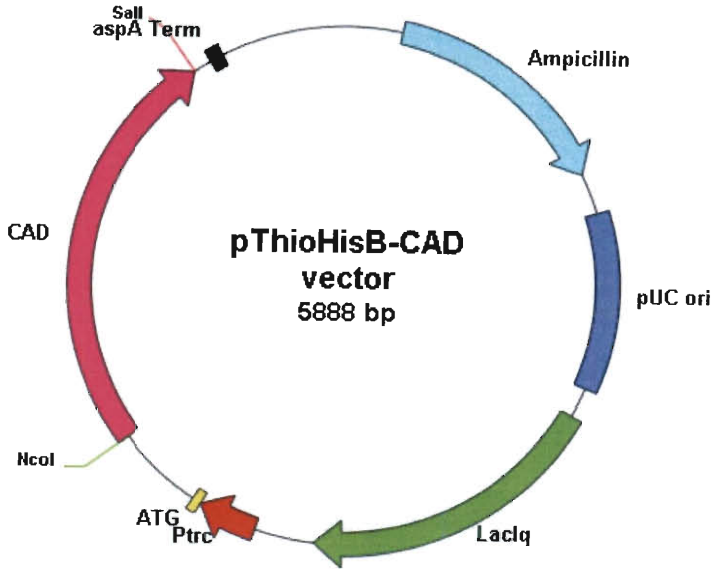

Figure 3.8 – Plasmid map of pThioHisB-*cad*
The *cad* gene was inserted into pThioHisB vector at NcoI and SalI sites.

3.4 Comparison of expression of constructed plasmids in various strains using different carbon sources

To systematically compare the expression of the *cad* gene from various vectors, the strains GNB11339 ($\Delta acnA{:}Km^R$) , GNB11315 (Chromosomal P_{ara}-*groEL/S*), and GNB11321 (Chromosomal $P_{A1/lacO-1}$-*dnaK/J-lacI*^{q}) were employed to characterize the expression rate of *cad* gene. GNB11339 is the strain MG1655 with an acnA mutation; without acnA, the CAD protein is expected to have more accessibility to *cis*-aconitate. Meanwhile, acnB is the main aconitase expressed during the exponential growth of *E. coli*; hereby, acnB is necessary for growth during the new inoculation of overnight cultures. GNB11315 and GNB11321 are both heat shock chaperone over-expression strains. Over-expression of heat shock protein would be expected to improve the folding of the CAD protein. If the experiments were successful, I would expect more IA in the supernatant would be formed by GNB11339 strain because only the acnB protein

competed with the CAD protein for *cis*-aconitate. The CAD protein has more opportunities to decarboxylate the *cis*-aconitate in the cytoplasm. Since heat shock protein usually improves the protein folding, a higher activity of the CAD protein would be expected in the CAD enzyme assay in vitro because more active CAD protein would be formed under the assistance of heat shock protein. As a result, a higher amount of IA in the supernatant would be expected due to the presence of more active CAD protein.

These strains bearing the plasmids were grown aerobically under the same conditions. Their ODs were measured to be identical when aliquots of cultures were taken. The supernatants were analyzed in the HPLC to determine the production yield of itaconate. Meanwhile, the *cis*-aconitate and citrate were utilized as the sole carbon sources to demonstrate the activity of CAD in vivo.

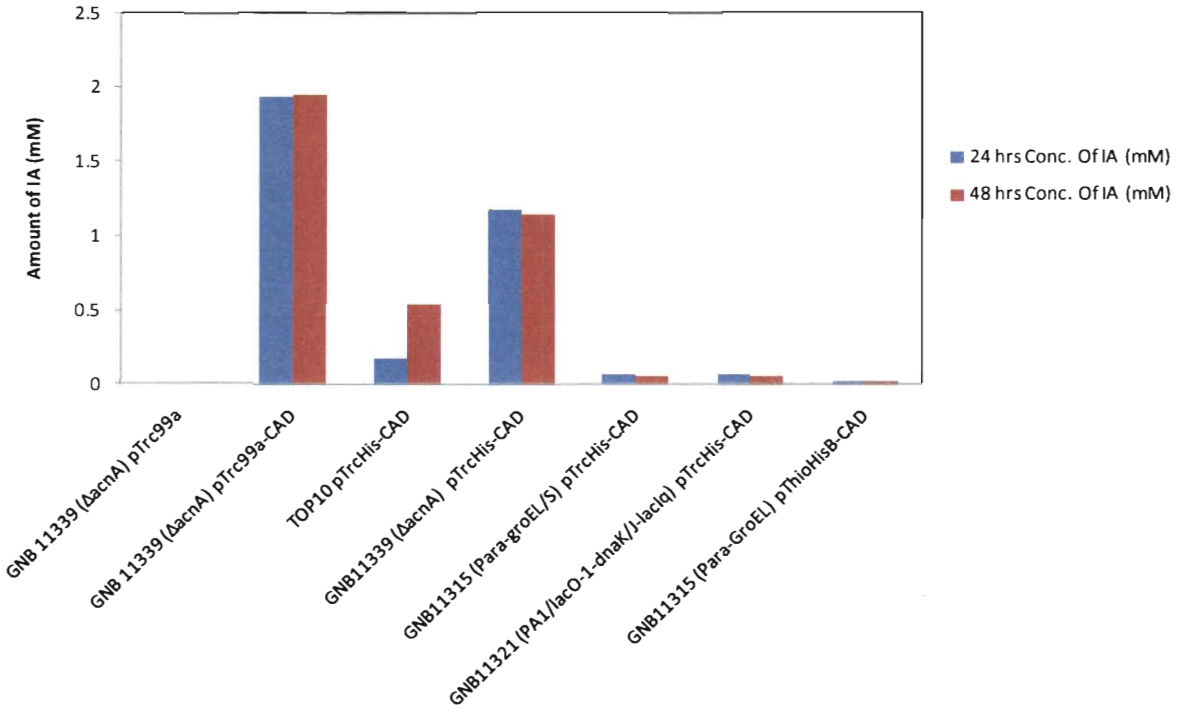

Figure 3.9 – Comparison of supernatant contents of various *E. coli* strains bearing different plasmids after 24 and 48 hrs incubation at 30°C.
During the aerobic inoculation, *cis*-aconitate was served as the sole external carbon sources. GNB11339 pTrc99a strain was used as experimental control.

In Figure 3.9, it is clear that GNB11339 pTrc99a-*cad* generated the highest amount of IA at each time point. As a control, GNB11339 pTrc99a with the *cad* insert didn't produce any IA as expect. Interestingly, in the same *E. coli* strain GNB11339, the enzyme expressed from pTrc99a-*cad* plasmid seemed to display higher catalytic activity than one from pTrcHis-*cad*. Moreover, various strains bearing the same pTrcHis-*cad* plasmid displayed different production rates of IA at each time period. But the strain GNB11339 was preferred since a higher amount of IA was generated. Surprisingly, the chaperone over-expression strains (GNB11315 and GNB11321) didn't improve IA production rate in the batch. These results suggest that pTrc99a-*cad* plasmid was a better one to express high active CAD protein and the Δ*acnA* mutant may provide advantages to *E. coli* in producing IA. Additionally, pThioHisB-*cad* may not express

CAD activity at all since the amount of IA detected in the assays of cells bearing this construct is so low in the supernatant.

To further confirm the results obtained from the previous trial, strains bearing various plasmids were tested in a new experiment. In this experiment, citrate replaced *cis*-aconitate as the carbon source because I wish to prove the previously verified route in a small scale: citrate→ *cis*-aconitate→ itaconate. The strains GNB11339 pTrc99a and BL21 were used as positive controls, while LB medium with citrate served as a negative control. The supernatant of each strain from 24 hrs incubation cultures was analyzed in HPLC. As shown in Figure 3.10, the strain GNB11339 pTrc99a-*cad* still displayed the highest yield of IA as expected. The highest amount of IA yield from pTrcHis-*cad* vector was also obtained from GNB11339 strain. This result further suggests the Δ*acnA* mutant allows CAD to compete more fiercely for *cis*-aconitate inside the cell.

Interestingly, the strain GNB11321 pThioHisB-*cad* displayed a better yield of IA than GNB11339 strain bearing the same plasmid. This result suggests that the over-expression of chaperon may increase the activity of enzyme. Additionally, the strain BL21 pET32a & pT-GroE also produced small quantity of IA. In summary, the plasmid pTrc99a-*cad* had presented the best yield of IA production in *E. coli* strain and the Δ*acnA* mutant improved the production rate of IA during the fermentation.

Furthermore, the data from both trials indicate that using *cis*-aconitate and citrate as the carbon sources, *E. coli* strains generated higher production of IA than ones using glucose (data not shown). This phenomenon was reasonable because *cis*-aconitate in the medium could be directly catalyzed by CAD and citrate could be converted to *cis*-aconitate more easily than

glucose. This result somehow illustrated the previously identified pathway: citrate→ *cis*-aconitate→ itaconate.

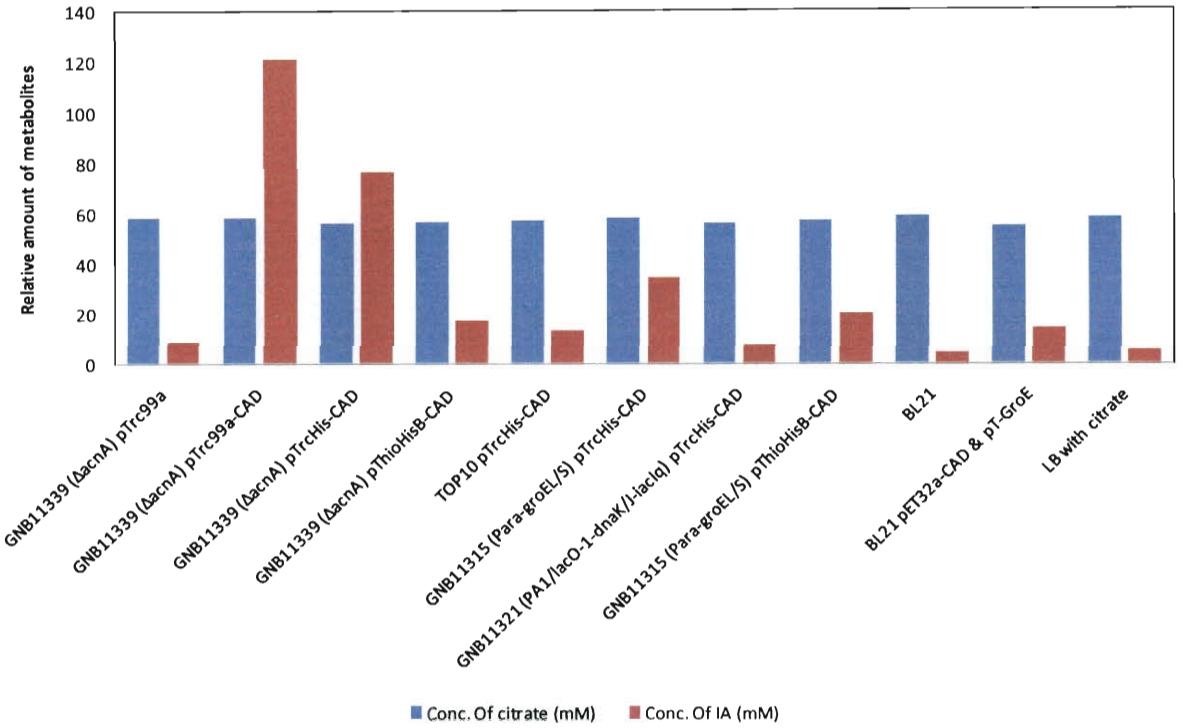

Figure 3.10 – Comparison of supernatant contents of cultures of various *E. coli* strains bearing different plasmids at 24 hrs incubation.
During the aerobic incubation, 60 mM citrate served as the sole external carbon sources. GNB11339 pTrc99a and BL21 strains were used as experimental controls and LB medium with citrate was used as negative control.

To compare the activity of CAD expressed from pTrcHis-cad and pTrc99a-cad in vitro, the strains TOP10 and GNB11321 were employed as the hosts. The cells were grown aerobically with or without induction of IPTG. Then after 4 hrs incubation, the cells were subject to sonication and cell lysates were analyzed in the CAD enzyme assay. As shown in the Figure 3.11, with induction of IPTG, the CAD expressed from pTrc99a-*cad* showed significantly higher activity than the one from pTrcHis-*cad*. This result further supports the previous conclusion that

pTrc99a-*cad* plasmid was a better one to express high active CAD protein, leading to the high yield of IA production in *E. coli* strains.

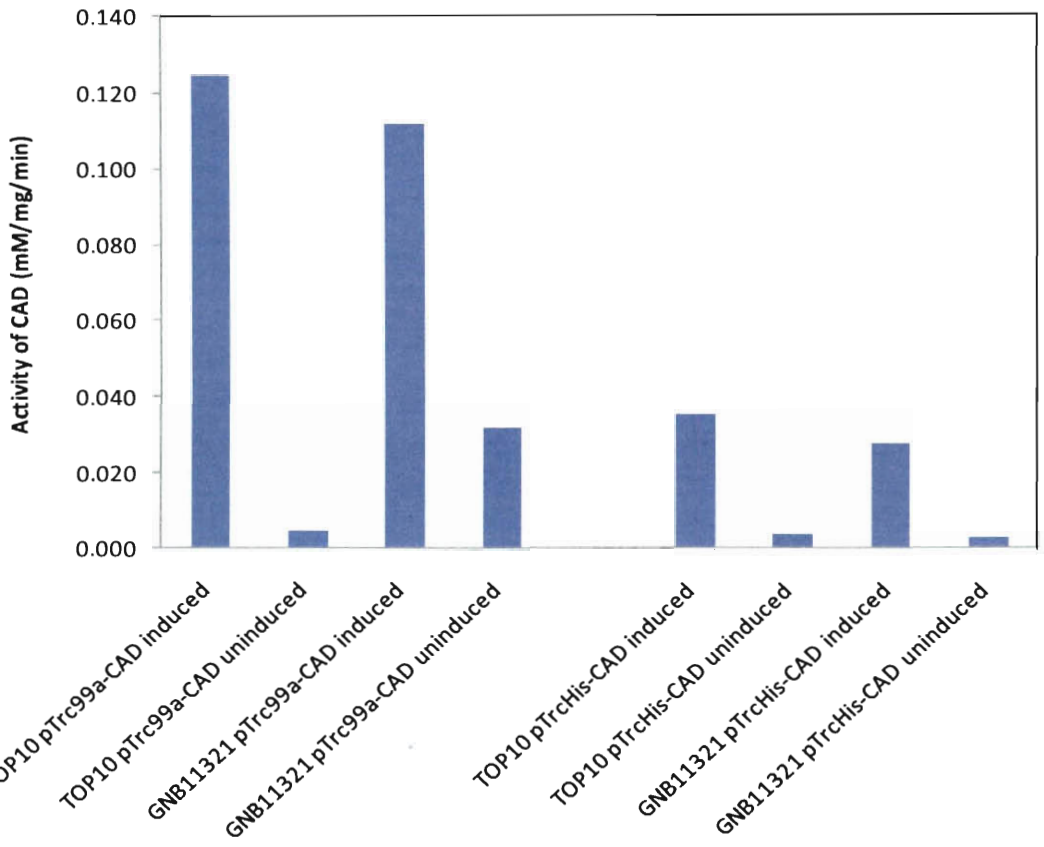

Figure 3.11 – Comparison of CAD activities from TOP10 and GNB11321 strains bearing either pTrc99a-*cad* or pTrcHis-*cad* under the presence or absence of 1mM IPTG.
The unit (mM/mg/min) is defined as 1 mM of IA produced from 1 mg of cell crude in the *cis*-aconitate enzymatic assay per min.

CHAPTER 4. Exploring the potential aconitase gene from Aspergillus species and Shewanella oneidensis

4.1 No "citrate dehydratase" existed in the supernatant of *Aspergillus niger (A. niger)*.

The main purpose of this experiment is to determine whether "citrate dehydratase" exists in the fungus to catalyze only between citrate and *cis*-aconitate. As mentioned in the background, "citrate dehydratase" was identified in *Aspergillus niger* strain 72-4. (Neilson, 1955, 1956) But La Nauze disproved Neilson's conclusions and showed that aconitase in *A. niger* strains 72-4 could both interconvert citrate or isocitrate to *cis*-aconitate. (La Nauze, 1966) However, it is ambiguous to determine whose conclusions are correct.

In this project, *Aspergillus niger* DSM872, which is closed to the strain used by Neilson, was grown for 2 days. Mycelia were filtered, freeze-dried, and grinded up in Hepes buffer. The ammonium sulfate procedures (Neilson, 1956) were utilized to precipitate the "citrate dehydratase" in cell crude. After dialysis of the enzyme, the activity of proteins from 25% to 42% ammonium sulfate saturation was analyzed in the aconitase assays. (La Nauze, 1966) According to Neilson, the 25% - 42% fraction displayed 48 times higher conversion rate in catalyzing *cis*-aconitate→citrate than *cis*-aconitate →isocitrate. However, in my study, when either 10mM citrate or isocitrate was utilized in the aconitase assay, the same quantity of *cis*-aconitate (0.008 mM) from the reaction mixture was detected in HPLC using a 210nm UV detector (see Figure 4.1). People may observe that aconitases from various species display higher Km for citrate than isocitrate (Brenda Enzyme) so that a lower amount of citrate was converted into *cis*-aconitate. But the proposed citrate hydratase should overcome this limitation to produce

more *cis*-aconitate since plenty of citrate was used in the aconitase assay. This result really raised the question about the existence of citrate hydratase in the publication of Neilson or there is a significant difference in the strain used.

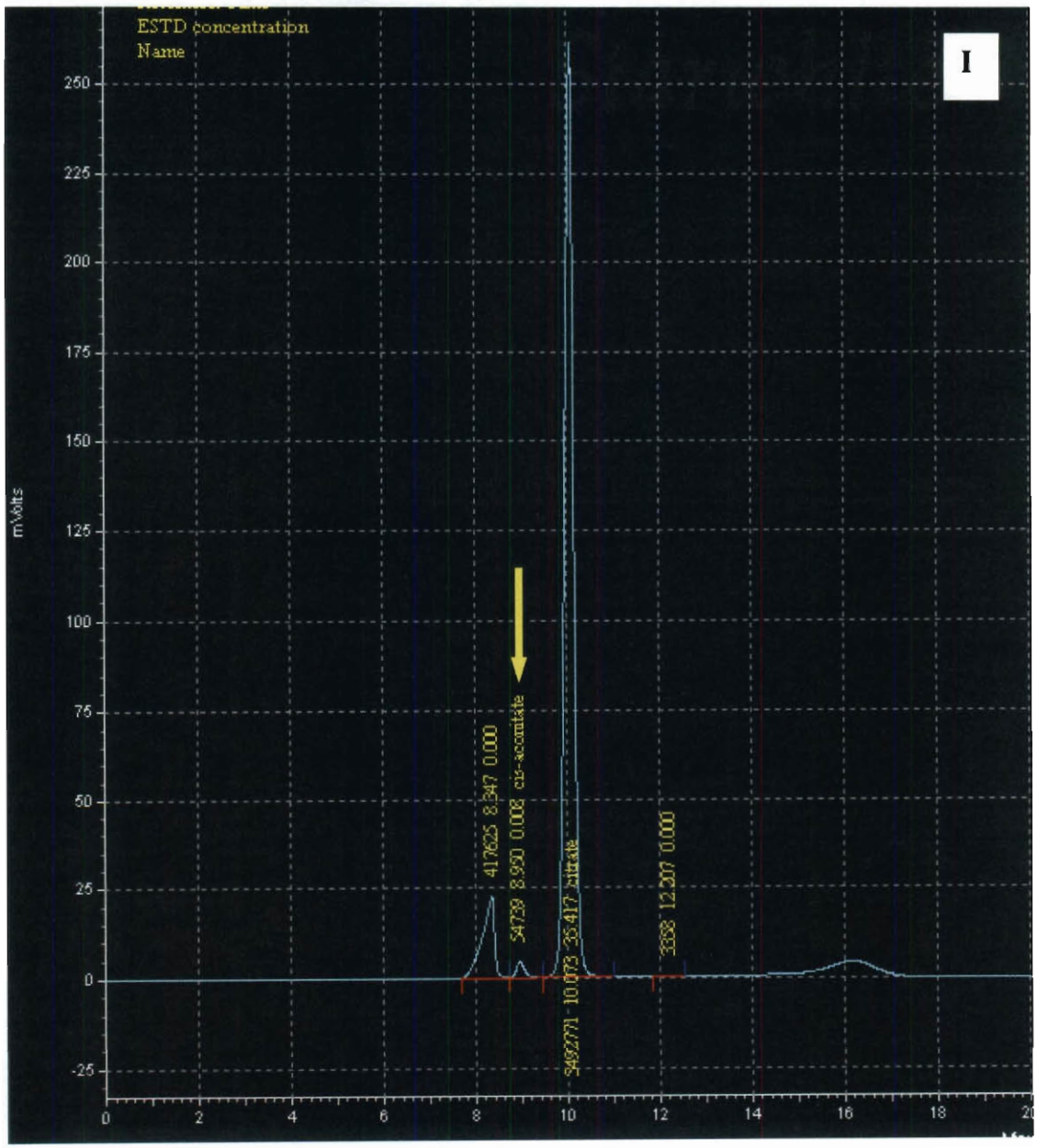

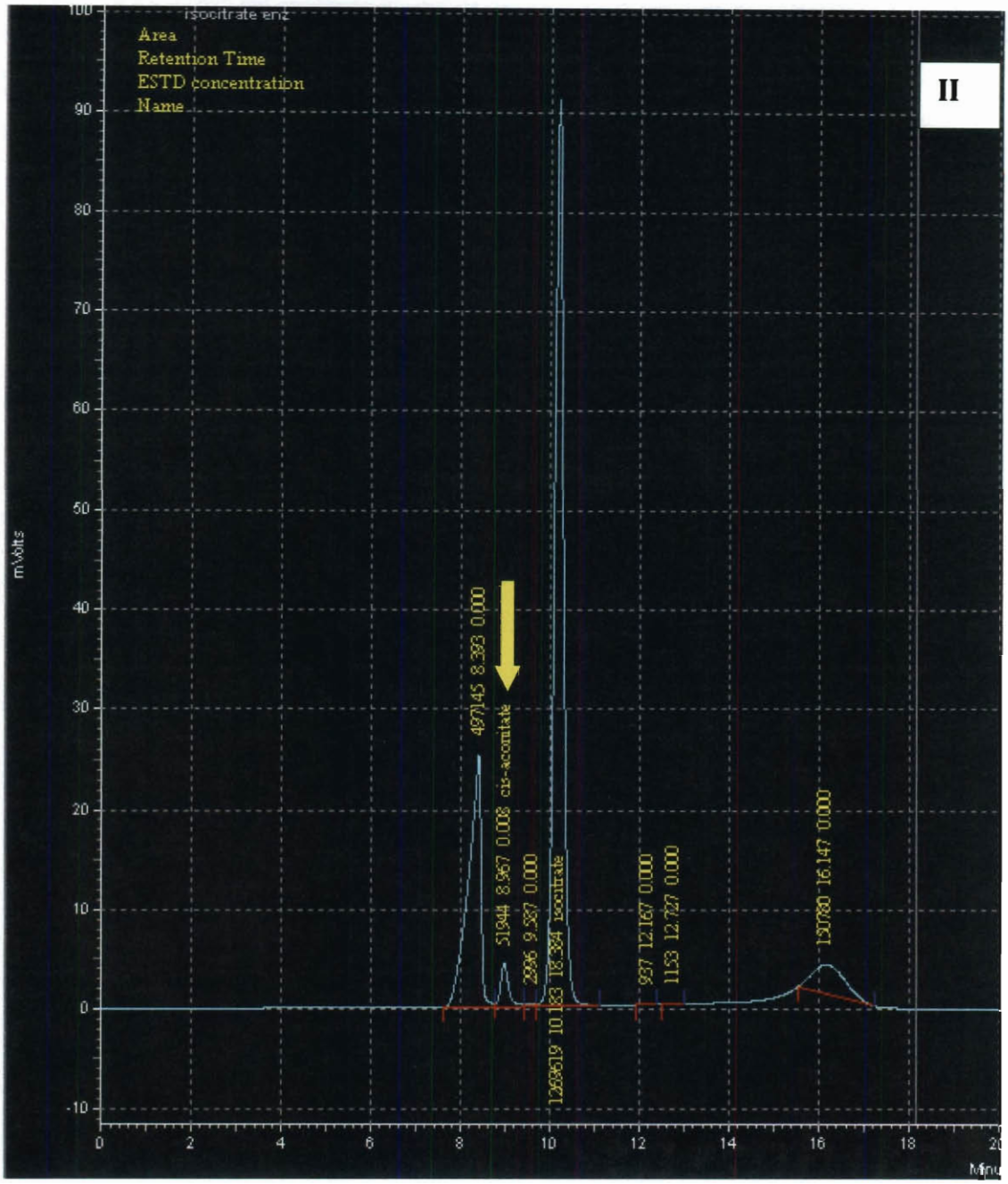

Figure 4.1 - Comparison of HPLC profiles from the aconitase assays of the 25%-42% fraction of *Aspergillus niger* cell crude.

(I) – The activated 25%-42% fraction reacts with 10mM citrate; **(II)** – The activated 25%-42% fraction reacts with 10mM isocitrate. Yellow arrow indicates the retention time for *cis*-aconitate in HPLC under 210 nm UV detector.

4.2 Explore the candidate aconitase genes from *Aspergillus terreus* NIH2624

Since no progression was made to identify the desired aconitase from *Aspergillus niger,* I planned to directly clone the aconitase genes from *A. terreus* by PCR. As mentioned in the introduction, bioinformatic analysis revealed four candidate aconitases gene from *A. terreus* NIH2624: ATEG_03325 (mitochondrial precursor) and ATEG_08913 (cytosolic precursor) under non-itaconic acid producing conditions; ATEG_02937 (mitochondrial precursor) and ATEG_05743 (cytosolic precursor) under itaconic acid producing conditions. To clone these genes, the mycelia of *A. terreus* NIH2624 were collected from 2 day incubation in CM medium with ammonium tartrate. The genomic DNA was extracted from the mycelia using the MasterPure™ Yeast DNA Purification kit (Epicentre Biotechnologies). Next, primers were designed to remove the introns from each gene.

4.3 Mitochondrial aconitate hydratase (ATEG_02937) from *Aspergillus terreus* NIH2624 was cloned into pTrc99a vector.

Three sets of primers were designed to clone the coding exons of ATEG_02937 gene from genomic DNA of *Aspergillus terreus* NIH2624; another set of PCR were performed to join all the coding exons and amplify the entire gene. The gene ATEG_02937 was annotated as "mAcn-ita" The cloned gene was successfully inserted into pTrc99a vector (Figure 4.2). Finally, the sequencing result reveals that the cloned gene matches exactly with the sequence of ATEG_02937 gene.

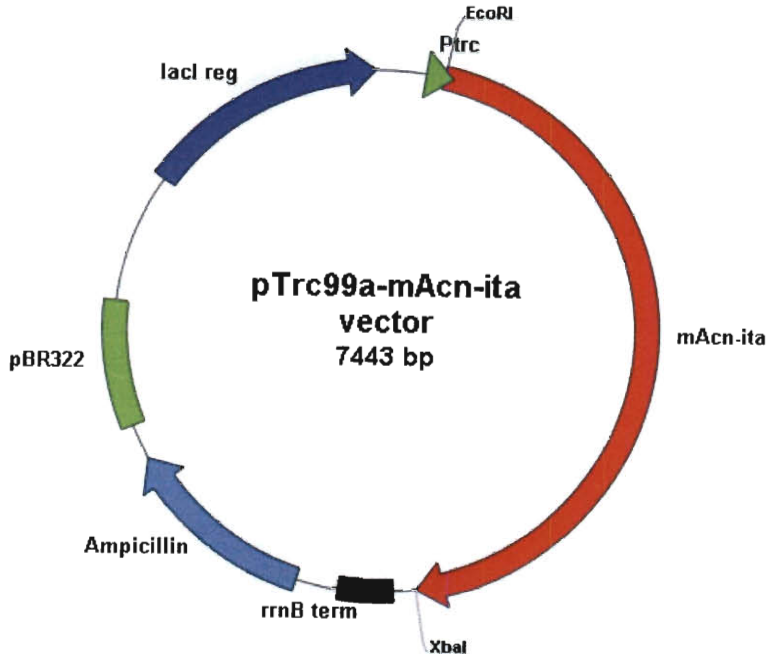

Figure 4.2 – Plasmid map of pTrc99a-mAcn-ita.
ATEG_02937 gene (mAcn-ita) will be inserted at EcoRI and XbaI sites.

Next, the plasmid pTrc99a-mAcn-ita was transformed into GNB11338 and GNB11339, respectively, while the vector pTrc99a was transformed into both strains as controls. All the strains grew in LB medium with 50 mM glucose under the same conditions in the aerobic shaking flask. After induction of IPTG, the supernatant of each strain was collected and analyzed at three time points: 4, 24, and 48 hours. As shown in Figure 4.3-I, comparing to the control, GNB11338 pTrc99a-mAcn-ita displayed a large peak at 10.3 min in the supernatant after 4 hours induction. However, after 24 and 48 hours induction, the peak at the same retention time from GNB11338 pTrc99a-mAcn-ita diminished to the same size as the peak at 10.3 min from the control GNB11338 pTrc99a. Meanwhile, comparing the supernatants from GNB11339 pTrc99a-mAcn-ita and GNB11339 pTrc99a, GNB11339 pTrc99a-mAcn-ita also displayed a large peak at 10.3 min after 4 hours induction. Interestingly, after 24 and 48 hrs induction, the peak at the

same retention time from GNB11339 pTrc99a-mAcn-ita also decreased to the same size as the peak at 10.3 min from the control GNB11339 pTrc99a (data not shown). All of these results strongly suggest that pTrc99a-mAcn-ita may be functional to express the inserted gene and the expressed mAcn-ita protein should be soluble in the cytoplasm. More importantly, this protein directly influences the content of metabolites at early stage after the induction.

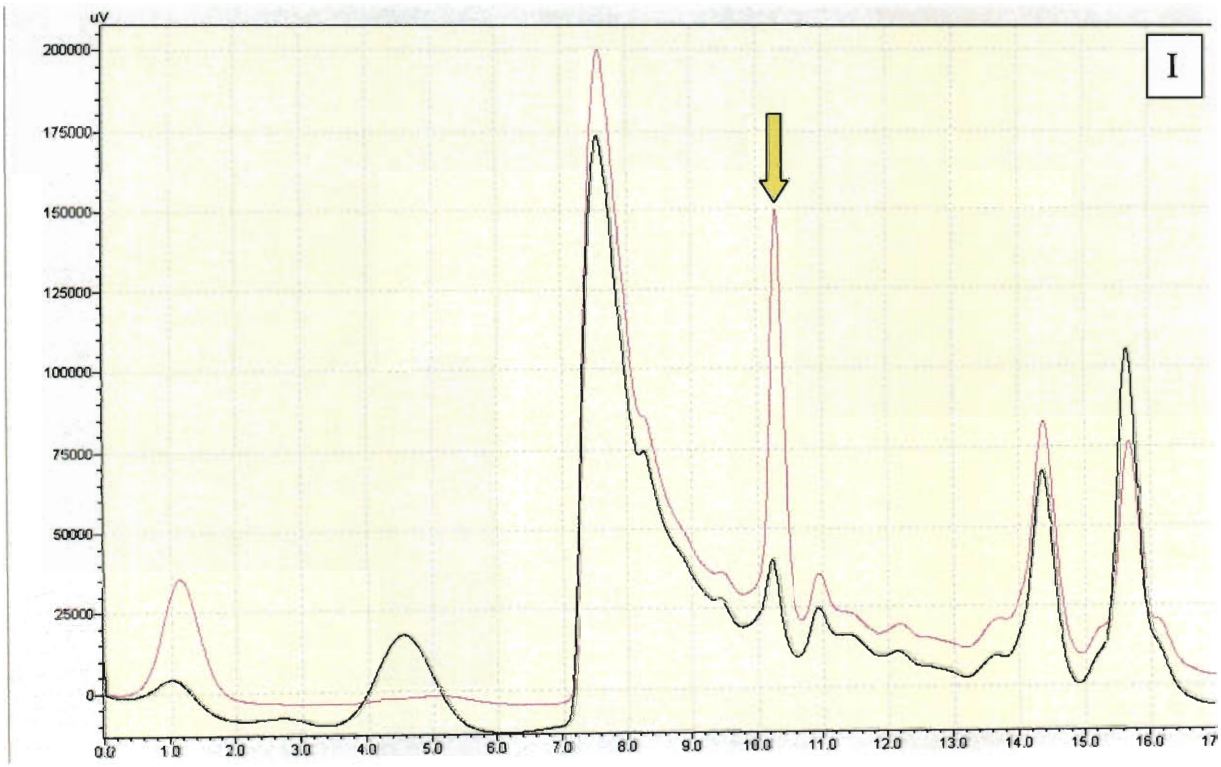

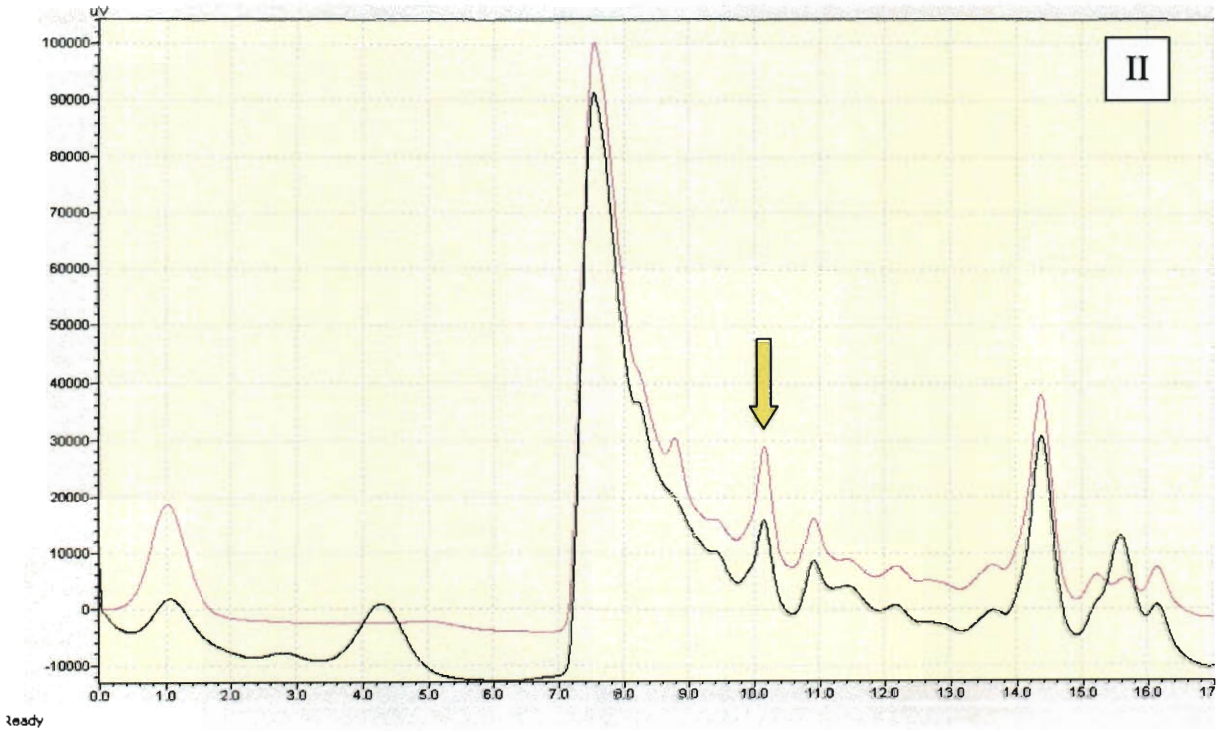
uV
100000
90000
80000
70000
60000
50000
40000
30000
20000
10000
0
-10000
0.0
1.0
2.0
3.0
4.0
5.0
6.0
7.0
8.0
9.0
10.0
11.0
12.0
13.0
14.0
15.0
16.0
17
II
Ready

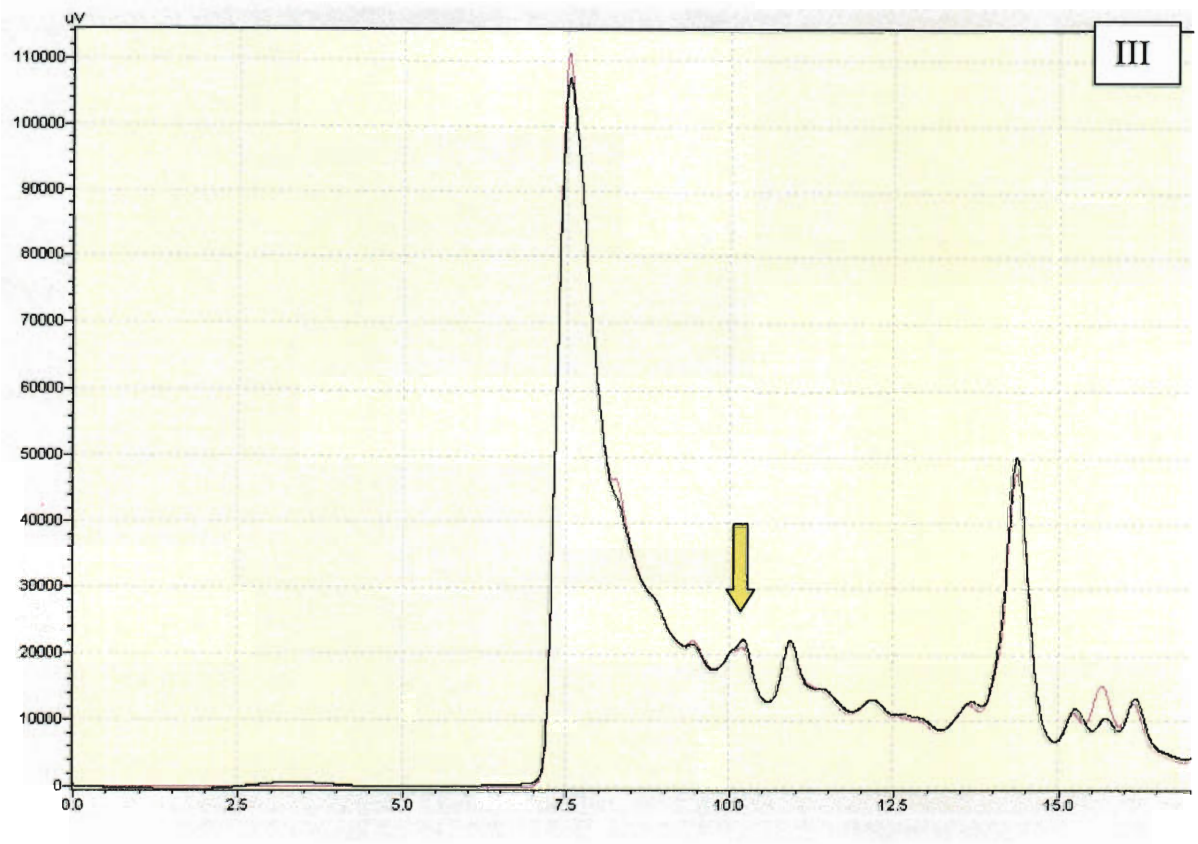

Figure 4.3 - Comparision of supernatants of GNB11338 pTrc99a and GNB11338 pTrc99a-mAcn-ita in HPLC.
The supernatant of each strain was collected after 4 hrs **(I),** 24 hrs **(II),** and 48 hrs **(III)** induction of IPTG. The black line represents the supernatant of GNB11338 pTrc99a; the pink line represents the supernatant of GNB11338 pTrc99a-mAcn-ita. Yellow arrow indicates the important peak at 10.3 min in HPLC.

4.4 Mitochondrial aconitate hydratase (ATEG_03325) and cytosolic aconitate hydratase (ATEG_08913) from *Aspergillus terreus* NIH2624 were cloned into pTrc99a vector, too.

Using the similar methods as cloning the gene ATEG_02937 from *A. terreus* NIH2624, five sets of primers were designed to clone the coding exons of ATEG_03325 gene, while eight pairs of primers were ordered to amplify the coding exons of ATEG_08913. For both genes, another trial of PCR was performed joined all the coding exons and amplified the entire gene.

The cloned gene was successfully inserted into pTrc99a vector and verified by sequencing (see Figure 4.4 and 4.5). Likewise, the plasmid pTrc99a-ATEG_03325 and pTrc99a-ATEG_08913 were transformed into GNB11338 and GNB11339, respectively, while the vector pTrc99a was transformed into both strains as controls. All the strains grew under the same conditions in the aerobic shaking flask. After induction of IPTG, the supernatant of each strain bearing each plasmid was collected at three time points: 4, 24, and 48 hours, and then analyzed in HPLC as before.

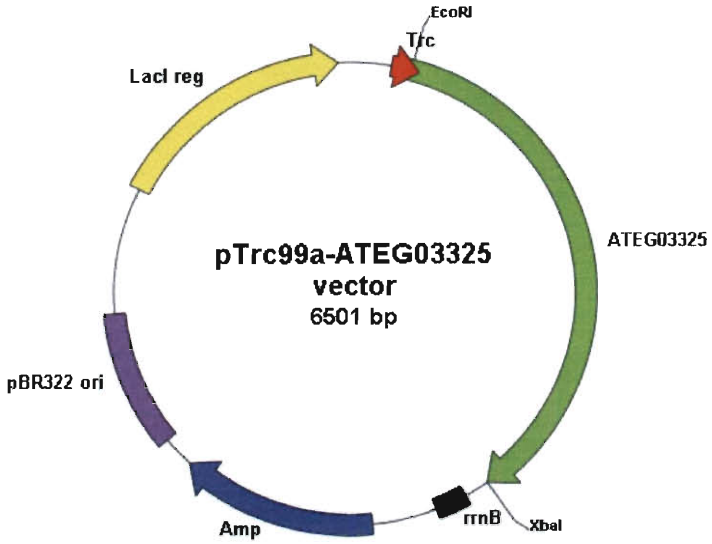

Figure 4.4 – Plasmid map of pTrc99a-ATEG03325.
The gene ATEG_03325 was inserted into pTrc99a vector at EcoRI and XbaI sites.

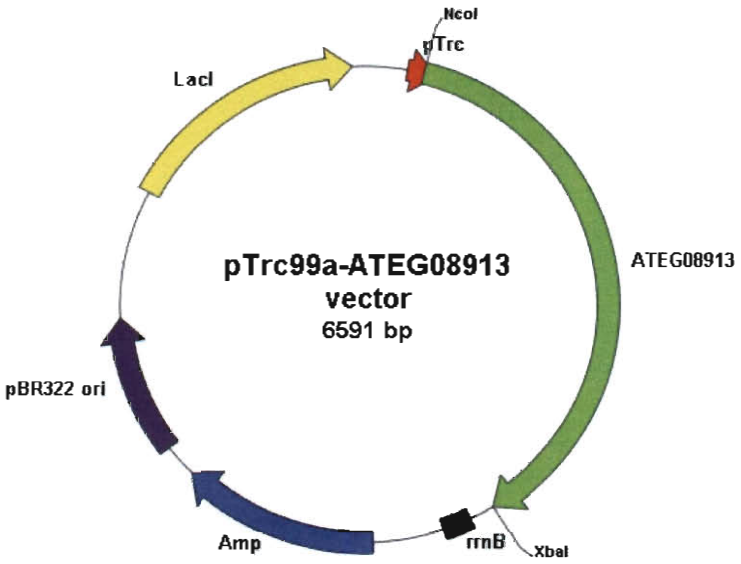

Figure 4.5 – Plasmid map of pTrc99a-ATEG08913.
The gene ATEG_08913 was inserted into pTrc99a vector at NcoI and XbaI sites.

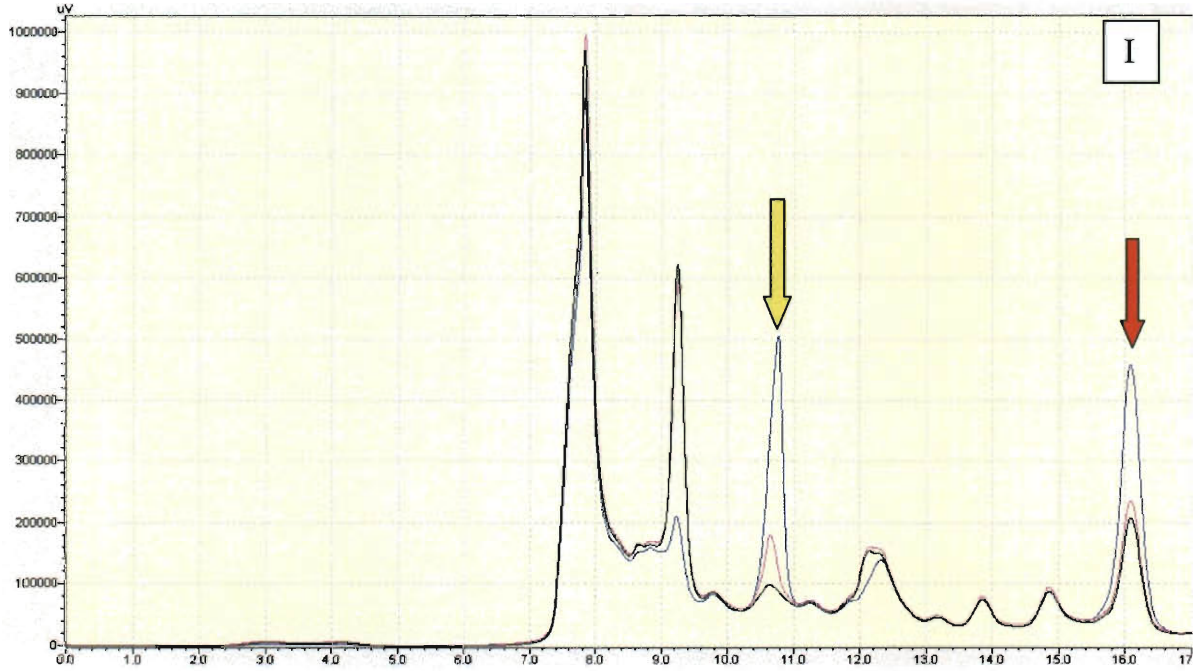
uV
1000000
900000
800000
700000
600000
500000
400000
300000
200000
100000
0
0.0
1.0
2.0
3.0
4.0
5.0
6.0
7.0
8.0
9.0
10.0
11.0
12.0
13.0
14.0
15.0
16.0
17
I

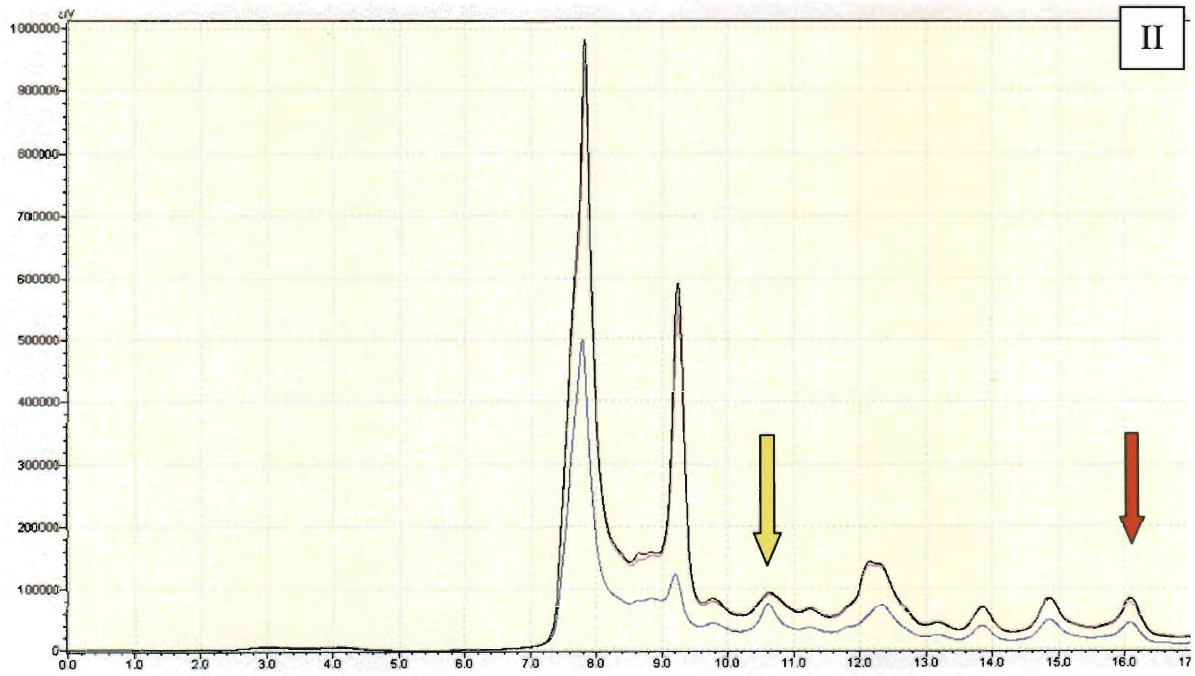
uV
1000000
900000
800000
700000
600000
500000
400000
300000
200000
100000
0
0.0
1.0
2.0
3.0
4.0
5.0
6.0
7.0
8.0
9.0
10.0
11.0
12.0
13.0
14.0
15.0
16.0
17
II

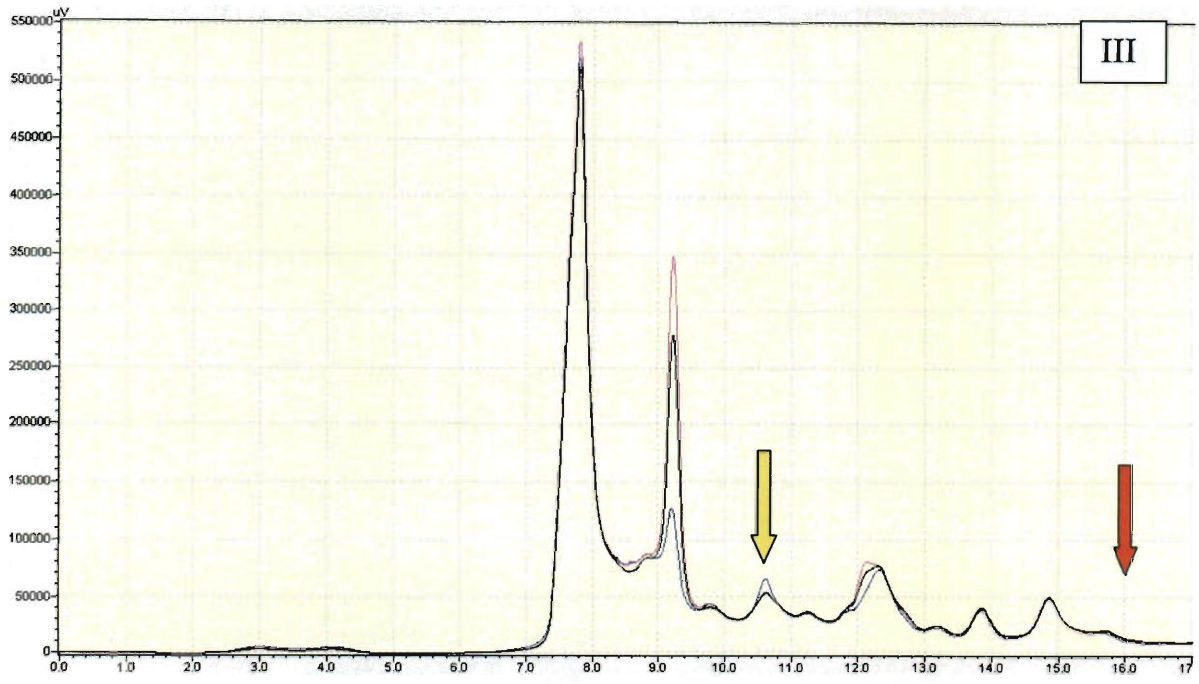

Figure 4.6 - Comparision of metabolite contents of supernatants from the strains GNB11338 pTrc99a, GNB11338 pTrc99a-ATEG03325, and GNB11339 pTrc99a-ATEG08913 in HPLC.
The supernatant of each strain was collected after 4 hrs **(I),** 24 hrs **(II),** and 48 hrs **(III)** induction of IPTG. The black line represents the supernatant of GNB11338 pTrc99a; the pink line represents the supernatant of GNB11338 pTrc99a-ATEG_03325; the blue line represents the supernatant from GNB11338 pTrc99a-ATEG_08913. Yellow arrow indicates the important peak at 10.3 min in HPLC. Red arrow indicates the important peak at 16.1 min in HPLC.

As shown in Figure 4.6-I, after 4 hrs induction of IPTG, GNB11338 bearing either pTrc99a-ATEG_03325 or pTrc99a-ATEG_08913 displayed a large peak at 10.3 min in the supernatant comparing to the control GNB11338 bearing the vector pTrc99a. Meanwhile, the peak at 10.3 min from GNB11338 pTrc99a-ATEG_08913 is much stronger than one at the same retention time from GNB11338 pTrc99a-ATEG_03325. Interestingly, GNB11338 bearing pTrc99a-ATEG_08913 also showed a big peak at 16.1 min in comparison to GNB11338 bearing either pTrc99a-ATEG_03325 or pTrc99a. However, after 24 and 48 hrs induction, the peak at 10.3 min from both GNB11338 pTrc99a-ATEG_03325 and GNB11338 pTrc99a-ATEG_08913

decreased to the same size as the peak at same retention time from the control GNB11338 pTrc99a. In addition, a peak at 16.1 min from GNB11338 bearing pTrc99a-ATEG_08913 also reduced to the same intensity as the peak from GNB11338 bearing either pTrc99a-ATEG_03325 or pTrc99a after 24 and 48 hrs induction.

Meanwhile, comparing the supernatants from GNB11339 pTrc99a-ATEG_03325, GNB11339 pTrc99a-ATEG_08913 and GNB11339 pTrc99a, GNB11339 strain expressing the cloned aconitase genes also displayed a large peak at 10.3 min in contrast to the control GNB11339 pTrc99a after 4 hours induction. Interestingly, after 24 and 48 hrs induction, the peak at the same retention time from GNB11339 strain bearing either pTrc99a-ATEG_03325 or pTrc99a-ATEG_08913 also decreased to the same size as the peak at 10.3 min from the control GNB11339 pTrc99a (data not shown). In addition, GNB11339 pTrc99a-ATEG_08913 also displayed a big peak at 16.1 min after 4 hrs induction comparing to the other two strains. The peak at 16.1 min from GNB11339 pTrc99a-ATEG_08913 decreased to the similar size as the other two strains after 24 and 48 hrs induction.

All these results suggest that both ATEG_03325 and ATEG_08913 proteins are soluble and functional in the cytoplasm of host cells. They both affected the content of metabolites in the early induction phase. More interestingly, ATEG_08913 protein seems to have a stronger influence than ATEG_03325.

4.5 No activity of CAD was observed from the strains bearing pPRP140-*cad* plasmid.

As shown in Table 2, *acnD* codes for a 2-methylcitrate dehydratase that seems to only catalyze the inter-conversion of citrate and *cis*-aconitate under the assistance of PrpF protein

(Grimek and Escalante-Semerena, 2004). It means that less *cis*-aconitate will be degraded to isocitrate so that *cis*-aconitate can be accumulated as the substrate for CAD. We were grateful to receive the plasmid pPRP140 coding for both AcnD and PrpF proteins from Dr. Escalante-Semerena. The plasmid was verified by restriction digests and sequencing. Initially, I transformed both pPRP140 and pDHC29-*cad* into the wild type strain. After induction of pDHC29-*cad*, no activity of CAD was detected using the *cis*-aconitate assay.

Alternatively, I digested the pTrcHis-*cad* vector to excise the fragment containing the *cad* gene and Lac Repressor ($lacI^q$), and then ligated the purified fragments into pPRP140. The new constructed plasmid was analyzed by PCR and confirmed by sequencing (Figure 4.5). Next, I transformed this plasmid into the parental strains. After induction of the *acnD, prpF, and cad* gene from the plasmid, I tested the activity of *CAD* expressed from this new plasmid. As an experimental control, the same parental strains bearing the pPRP140-*cad* were incubated without the induction of plasmid overtime. As a control, the same parental strains bearing the pTrcHis-*cad* plasmid were used for the comparison. In the CAD enzyme assay, no significant CAD activity was detected. This result indicates that the new construct may not function properly or the growth conditions were not optimal for the protein folding. More work will be needed to trouble-shoot the problems.

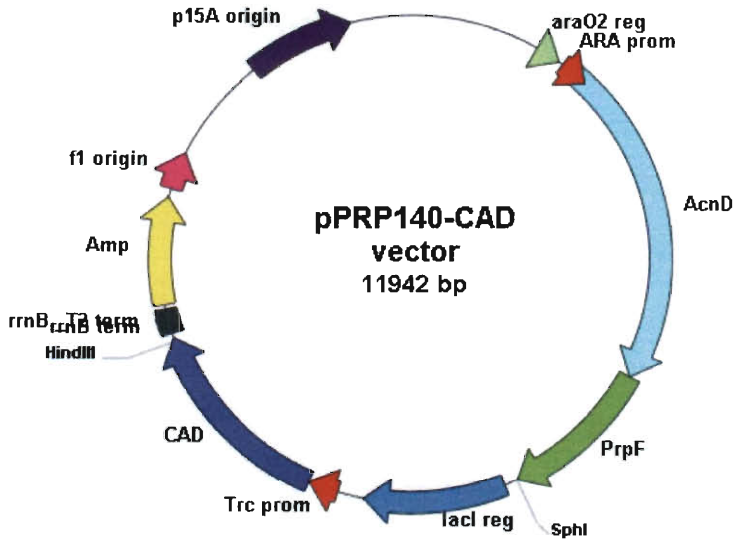

Figure 4.7 – The gene map of pPRP140-*cad*.
The plasmid is ampicillin resistant and originates from the pBAD30. The *acnD and prpF* genes are induced by arabinose, whereas the *cad* gene is induced by IPTG.

Chapter 5. Conclusions

Recent studies have examined the potential of *E. coli* as a host to produce itaconic acid. Itaconic acid is a valuable renewable chemical used frequently in the medicine, pharmacy, and industry. Previous studies have verified the metabolite pathway of IA production and revealed the unique characteristics of *cis*-aconitate decarboxylase (*cad)* gene. In this study, I explored the expression of *cad* gene in *E.* coli. The CAD enzyme is soluble in the cytoplasm and active in catalyzing *cis*-aconitate to itaconate both in vitro and in vivo. Various vectors, including pTrc99a, pTrcHis, pDHC29, pET32a, and pThioHisB, were employed to over-express *cad* gene. So far, highest amount of IA from supernatant and best activity of CAD in vitro were obtained from the strains bearing pTrc99a-*cad* plasmid. The mutation of the *acnA* or *acnB* gene in the host *E. coli* seems to improve the production of IA comparing to the wild type strains. In particular, when 60mM citrate was utilized as the sole carbon source in the batch, the strain GNB11339 bearing pTrc99a-*cad* yielded highest amount of IA in the supernatant.

The low supply of *cis*-aconitate in the cytoplasm is one limitation in this project. To enhance the conversion of citrate to *cis*-aconitate, the candidate genes of aconitases from *Aspergillus terreus* were explored in the project. The mitochondrial and cytosolic aconitate hydratases (ATEG_02937, ATEG_03325 and ATEG_08913) have been successfully cloned and expressed from pTrc99a vector. After four-hour induction of IPTG, the strong peak at 10.3 min appeared in the supernatant from the strains expressing the aconitate hydratases. However, after a long time induction, this strong peak abated to the same concentration as the peak observed in the control. Surprisingly, the strain GNB11338 pTrc99a-ATEG_08913 also showed a big peak at 16.1 min at the early induction stage. Therefore, all cloned aconitases are active in catalyzing the

metabolites inside the cytoplasm. Although I haven't identified the content of this large peak at 10.3 min in HPLC, it is certain that the cloned genes stressed expression of certain metabolites in various degrees. If the peak at 10.3 min is verified to be *cis*-aconitate, this obtained data will support my hypothesis that certain aconitases from *A. terreus* could accumulate significant amount of *cis*-aconitate inside the cytoplasm. Consequently, I expect that a higher amount of IA will be achieved when high levels of CAD protein is co-expressed with this aconitase in the *E. coli*. In addition, I would like to continue to analyze the expression of the rest of aconitase genes to determine whether they can also enhance the production of *cis*-aconitate.

References

Beinert, H., and Kennedy, M.C. (1993a). Aconitase, a 2-Faced Protein - Enzyme and Iron Regulatory Factor. Faseb J *7*, 1442-1449.

Beinert, H., and Kennedy, M.C. (1993b). Aconitase, a two-faced protein: enzyme and iron regulatory factor. Faseb J *7*, 1442-1449.

Bennett, B., Gruer, M.J., Guest, J.R., and Thomson, A.J. (1995). Spectroscopic characterisation of an aconitase (AcnA) of Escherichia coli. Eur J Biochem *233*, 317-326.

Bentley, R., and Thiessen, C.P. (1955). Cis-Aconitic Decarboxylase. Science *122*, 330-330.

Bentley, R., and Thiessen, C.P. (1957a). Biosynthesis of itaconic acid in Aspergillus terreus. I. Tracer studies with C14-labeled substrates. J Biol Chem *226*, 673-687.

Bentley, R., and Thiessen, C.P. (1957b). Biosynthesis of itaconic acid in Aspergillus terreus. II. Early stages in glucose dissimilation and the role of citrate. J Biol Chem *226*, 689-701.

Bentley, R., and Thiessen, C.P. (1957c). Biosynthesis of itaconic acid in Aspergillus terreus. III. The properties and reaction mechanism of cis-aconitic acid decarboxylase. J Biol Chem *226*, 703-720.

Betancourt, T., Pardo, J., Soo, K., and Peppas, N.A. Characterization of pH-responsive hydrogels of poly(itaconic acid-g-ethylene glycol) prepared by UV-initiated free radical polymerization as biomaterials for oral delivery of bioactive agents. Journal of Biomedical Materials Research Part A *93A*, 175-188.

Blatt, A.H. (1943). Organic syntheses, Vol II (Wiley, New York).

Bonnarme, P., Gillet, B., Sepulchre, A.M., Role, C., Beloeil, J.C., and Ducrocq, C. (1995). Itaconate biosynthesis in Aspergillus terreus. J Bacteriol *177*, 3573-3578.

Brock, M., Maerker, C., Schutz, A., Volker, U., and Buckel, W. (2002). Oxidation of propionate to pyruvate in Escherichia coli - Involvement of methylcitrate dehydratase and aconitase. European Journal of Biochemistry *269*, 6184-6194.

Coutinho, E., Cardoso, M.V., De Munck, J., Neves, A.A., Van Landuyt, K.L., Poitevin, A., Peumans, M., Lambrechts, P., and Van Meerbeek, B. (2009). Bonding effectiveness and interfacial characterization of a nano-filled resin-modified glass-ionomer. Dent Mater *25*, 1347-1357.

Cunningham, L., Gruer, M.J., and Guest, J.R. (1997). Transcriptional regulation of the aconitase genes (acnA and acnB) of Escherichia coli. Microbiology *143 (Pt 12)*, 3795-3805.

Dwiarti, L., Yamane, K., Yamatani, H., Kahar, P., and Okabe, M. (2002). Purification and characterization of cis-aconitic acid decarboxylase from Aspergillus terreus TN484-M1. J Biosci Bioeng *94*, 29-33.

Eimhjellen, K.E., and Larsen, H. (1955). The mechanism of itaconic acid formation by Aspergillus terreus. 2. The effect of substrates and inhibitors. Biochem J *60*, 139-147.

Frishman, D., and Hentze, M.W. (1996). Conservation of aconitase residues revealed by multiple sequence analysis. Implications for structure/function relationships. Eur J Biochem *239*, 197-200.

Gardner, P.R., Costantino, G., and Salzman, A.L. (1998). Constitutive and adaptive detoxification of nitric oxide in Escherichia coli. Role of nitric-oxide dioxygenase in the protection of aconitase. J Biol Chem *273*, 26528-26533.

Gardner, P.R., Costantino, G., Szabo, C., and Salzman, A.L. (1997). Nitric oxide sensitivity of the aconitases. J Biol Chem *272*, 25071-25076.

Gardner, P.R., and Fridovich, I. (1991). Superoxide sensitivity of the Escherichia coli aconitase. J Biol Chem *266*, 19328-19333.
Gardner, P.R., and Fridovich, I. (1992). Inactivation-reactivation of aconitase in Escherichia coli. A sensitive measure of superoxide radical. J Biol Chem *267*, 8757-8763.
Garvey, G.S., Rocco, C.J., Escalante-Semerena, J.C., and Rayment, I. (2007). The three-dimensional crystal structure of the PrpF protein of Shewanella oneidensis complexed with trans-aconitate: Insights into its biological function. Protein Science *16*, 1274-1284.
Grimek, T.L., and Escalante-Semerena, J.C. (2004). The acnD genes of Shewenella oneidensis and Vibrio cholerae encode a new Fe/S-dependent 2-methylcitrate dehydratase enzyme that requires prpF function in vivo. J Bacteriol *186*, 454-462.
Gruer, M.J., Artymiuk, P.J., and Guest, J.R. (1997a). The aconitase family: three structural variations on a common theme. Trends Biochem Sci *22*, 3-6.
Gruer, M.J., Bradbury, A.J., and Guest, J.R. (1997b). Construction and properties of aconitase mutants of Escherichia coli. Microbiology *143 (Pt 6)*, 1837-1846.
Gruer, M.J., and Guest, J.R. (1994). Two genetically-distinct and differentially-regulated aconitases (AcnA and AcnB) in Escherichia coli. Microbiology *140 (Pt 10)*, 2531-2541.
Guisbert, E., Herman, C., Lu, C.Z., and Gross, C.A. (2004). A chaperone network controls the heat shock response in E. coli. Genes Dev *18*, 2812-2821.
Holdom, K.S., and Winskill, N. (1988). Fermentation process and microorganism for producing aconitic acid (United States, Pfizer Inc. (New York, NY)).
Horswill, A.R., and Escalante-Semerena, J.C. (1999). Salmonella typhimurium LT2 catabolizes propionate via the 2-methylcitric acid cycle. Journal of Bacteriology *181*, 5615-5623.
Jaklitsch, W.M., Kubicek, C.P., and Scrutton, M.C. (1991). The Subcellular Organization of Itaconate Biosynthesis in Aspergillus-Terreus. J Gen Microbiol *137*, 533-539.
Jarry, A., and Seraudie, Y. (1995). Production of itaconic acid by fermentation (United States, Rhone-poulenc, Chimi).
Jordan, P.A., Tang, Y., Bradbury, A.J., Thomson, A.J., and Guest, J.R. (1999). Biochemical and spectroscopic characterization of Escherichia coli aconitases (AcnA and AcnB). Biochem J *344 Pt 3*, 739-746.
Kanamasa, S., Dwiarti, L., Okabe, M., and Park, E.Y. (2008). Cloning and functional characterization of the cis-aconitic acid decarboxylase (CAD) gene from Aspergillus terreus. Appl Microbiol Biotechnol *80*, 223-229.
Kinoshita, K. (1932). Über die Produktion von Itaconsäure und Mannit durch einen neuen Schimmelpilz Aspergillus itaconicus. . Acta Phytochim *5*, 271-287.
Kubicek, C.P., and Rohr, M. (1985). Aconitase and citric acid fermentation by Aspergillus niger. Appl Environ Microbiol *50*, 1336-1338.
La Nauze, J.M. (1966). Aconitase and isocitric dehydrogenases of Aspergillus niger in relation to citric acid production. J Gen Microbiol *44*, 73-81.
Lancashire, F. (1969). SOAP COMPOSITIONS HAVING IMPROVED CURD-DISPERSING PROPERTIES (PROCTER & GAMBLE).
Lauble, H., Kennedy, M.C., Beinert, H., and Stout, C.D. (1992). Crystal structures of aconitase with isocitrate and nitroisocitrate bound. Biochemistry-Us *31*, 2735-2748.
Lauble, H., Kennedy, M.C., Beinert, H., and Stout, C.D. (1994). Crystal structures of aconitase with trans-aconitate and nitrocitrate bound. J Mol Biol *237*, 437-451.
Ltd, C.I. (2008). Renewable chemicals.

Moshaverinia, A., Roohpour, N., Darr, J.A., and Rehman, I.U. (2009). Synthesis and characterization of a novel N-vinylcaprolactam-containing acrylic acid terpolymer for applications in glass-ionomer dental cements. Acta Biomater *5*, 2101-2108.

Neilson, N.E. (1955). The aconitase of Aspergillus niger. Biochim Biophys Acta *17*, 139-140.

Neilson, N.E. (1956). The presence of aconitase and aconitic hydrase in Aspergillus niger. J Bacteriol *71*, 356-361.

Okabe, M., Lies, D., Kanamasa, S., and Park, E.Y. (2009). Biotechnological production of itaconic acid and its biosynthesis in Aspergillus terreus. Appl Microbiol Biotechnol *84*, 597-606.

Panakova, M., Maassen, N., Zimmermann, M., Bölker, M., and Klinner, U. (2009). High-level formation of itaconic acid by the fungus Ustilago maydis. New Biotechnology *25*, 270.

Pfeifer, V.F., Vojnovich, C., and Heger, E.N. (1952). Itaconic Acid by Fermentation with Aspergillus Terreus. Ind Eng Chem *44*, 2975-2980.

Phillips, G.J., Park, S.K., and Huber, D. (2000). High Copy Number Plasmids Compatible with Commonly Used Cloning Vectors. BioTechniques *28*, 400-408.

Shadel, G.S. (2005). Mitochondrial DNA, aconitase 'wraps' it up. Trends Biochem Sci *30*, 294-296.

Shimi, I.R., and Nour El Dein, M.S. (1962). Biosynthesis of itaconic acid by aspergillus terreus. Arch Mikrobiol *44*, 181-188.

Tabuchi, T. (1991). Manufacture of itaconic acid with Ustilago. (Japan).

Tabuchi, T., Nakahara, T., (1980). Preparation of itaconic acid (Japan).

Tabuchi, T., Sugisawa, T., Ishidori, T., Nakahara, T., and Sugiyama, J. (1981). Itaconic Acid Fermentation by a Yeast Belonging to the Genus Candida. Agr Biol Chem Tokyo *45*, 475-479.

Tang, Y., Guest, J.R., Artymiuk, P.J., and Green, J. (2005). Switching aconitase B between catalytic and regulatory modes involves iron-dependent dimer formation. Mol Microbiol *56*, 1149-1158.

Tate, B.E. (1970). Itaconic acid, itaconic esters, and related compounds. High Polymers *24*, 205-261.

Teijon, C., Guerrero, S., Olmo, R., Teijon, J.M., and Blanco, M.D. (2009). Swelling properties of copolymeric hydrogels of poly(ethylene glycol) monomethacrylate and monoesters of itaconic acid for use in drug delivery. J Biomed Mater Res B Appl Biomater *91*, 716-726.

Tsuchiya, D., Shimizu, N., and Tomita, M. (2009). Cooperativity of two active sites in bacterial homodimeric aconitases. Biochem Bioph Res Co *379*, 485-488.

Van Der, W.M.J., and Caspers, M.P.M. (2007). Production of itaconic acid by fermentation (Nederlandse, Organisatie Voor Toegepast- Natuurwetenschappelijk Onderzoek Tno (Schoemakerstraat 97, 2628 VK Delft, NL)).

Varghese, S., Tang, Y., and Imlay, J.A. (2003). Contrasting sensitivities of Escherichia coli aconitases A and B to oxidation and iron depletion. J Bacteriol *185*, 221-230.

Volz, K. (2008). The functional duality of iron regulatory protein 1. Curr Opin Struct Biol *18*, 106-111.

Williams, C.H., Stillman, T.J., Barynin, V.V., Sedelnikova, S.E., Tang, Y., Green, J., Guest, J.R., and Artymiuk, P.J. (2002). E. coli aconitase B structure reveals a HEAT-like domain with implications for protein-protein recognition. Nat Struct Biol *9*, 447-452.

Willke, T., and Vorlop, K.D. (2001). Biotechnological production of itaconic acid. Appl Microbiol Biotechnol *56*, 289-295.

Winskill, N. (1983). Tricarboxylic-Acid Cycle Activity in Relation to Itaconic Acid Biosynthesis by Aspergillus-Terreus. J Gen Microbiol *129*, 2877-2883.

Yahiro, K., Takahama, T., Park, Y.S., and Okabe, M. (1995). Breeding of Aspergillus-Terreus Mutant Tn-484 for Itaconic Acid Production with High-Yield. J Ferment Bioeng *79*, 506-508.

Zhao, C.-L., Roser, J., Dersch, R., and Baumstark, R. (2004). DISPERSION RESINS CONTAINING ITACONIC ACID FOR IMPROVING WET ABRASION RESISTANCE (United States, BASF Aktiengesellschaft).

Zheng, L., Kennedy, M.C., Beinert, H., and Zalkin, H. (1992). Mutational analysis of active site residues in pig heart aconitase. J Biol Chem *267*, 7895-7903.

Appendix A

Complete medium for *Aspergillus* species From Dr. Greg May's Lab at MD Anderson Cancer Center in Houston, TX

Minimal Medium
50X MM Salts

Component	Amt./Liter
$NaNO_3$	300 gram
KCl	26 gram
$MgSO_4:7H_2O$	24.65 gm

Dissolve each in the order given and store at room temperature over a few drops of chloroform.

1M Phosphate Buffer pH~6.8

Component	Amt./Liter
KH_2PO_4	68 gm
K_2HPO_4	87.1 gm

Making Minimal Medium (MM)

Component	Amt./Liter
50X Salts	20 ml
Dextrose	10 gm for plates or 3.6 gm for liquid
1M KPO_4 pH6.8*	12 ml* Add after autoclaving for liquid media to prevent precipitate forming.
Trace Elements	1 ml
Agar	12.5 gm For solid media

Complete Medium (CM)

Add the following to MM.

Component	Amt./Liter
Yeast Extract	1 gm
Peptone	2 gm
Tryptone	1 gm
Vitamin Mix	2 ml
CM Supplement	10 ml

Greg's Modified Trace Elements

Component	Amt/Liter	mM
0.25 M EDTA pH8.0	100 ml	25
$FeSO_4:7H_2O$	1 gm	3.6
$ZnSO_4:7H_2O$	8.8 gm	30.1
$CuSO_4:5H_2O$	0.4 gm	1.6
$MnSO_4:H_2O$	0.15 gm	0.89
$Na_2B_4O_7:10H_2O$	0.1 gm	0.26
$NaMoO_4:2H_2O$	0.1 gm	0.41
$CaCl_2:2H_2O$	0.1 gm	0.68

Dissolve each in the indicated order being sure that the first is fully dissolved before adding the next. This is 1000 fold concentrated. Store the mixture at room temperature.

VITAMIN MIX

Component	Amt./Liter
p-Aminobenzoic acid	1 gm
Niacin	1 gm
Pyridoxine HCl	1 gm
Riboflavin	1 gm
Thiamine HCl	1 gm
Choline HCl	1 gm
d-Biotin	2 mg

Store at 4°C in the dark after autoclaving.

CM SUPPLEMENT

Component	Amt./Liter
Adenine HCl	5 gm
L-Methionine	5 gm
L-Lysine or Arginine	36.5 gm
Riboflavin	0.5 gm

Store at 4°C in the dark after autoclaving.